Nuclear Export of hnRNP Hrp1p and Nuclear Export of hnRNP Npl3p Are Linked and Influenced by the Methylation State of Npl3p

Chong Xu and Michael F. Henry*

Department of Molecular Biology, University of Medicine and Dentistry New Jersey-School of Osteopathic Medicine, Stratford, New Jersey

Eukaryotic mRNA processing and export are mediated by a series of complexes composed of heterogeneous nuclear ribonucleoproteins (hnRNPs). Many of these hnRNPs are methylated at arginine residues within their RGG domains. Although cellular arginine methylation is required for the efficient nuclear export of several hnRNPs, its role in this process is unknown. To address this question, we replaced the methylated RGG tripeptides of two hnRNPs, Npl3p and Hrp1p, with KGG. We found that these substitutions specifically abolish their methylation but have different effects on their nuclear export activity. Although the efficient export of Hrp1p requires cellular methyltransferase activity, the modification of Hrp1p itself is dispensable. In contrast, we found that Npl3 arginine methylation not only facilitates its own export but also is required for Hrp1p to efficiently exit the nucleus. Consistent with this observation, we found that Npl3p and Hrp1p exist in a ribonucleoprotein complex. We provide the first evidence that the arginine methylation of a particular protein directly affects its activity. Efficient export does not require methylation per se, but unmethylated arginine residues lead to retention of hnRNPs. Thus, arginine methylation serves to mask the Npl3p RGG domain for efficient ribonucleoprotein export.

When pre-mRNAs emerge from the transcription complex and throughout the time they are in the nucleus, they are associated with specific RNA-binding proteins, collectively referred to as heterogeneous nuclear ribonucleoproteins (hnRNPs) (5). hnRNPs are associated with pre-mRNAs starting at transcription and are proposed to function in nearly all the known steps of RNA maturation and nuclear export. Many of them remain bound to the resulting mRNAs during export and shuttle between the cytoplasm and the nucleus. This complex is further transformed until a distinct mRNA protein complex emerges in the cytoplasm to engage the translation machinery. Thus, ribonucleoprotein complexes are the functional forms in which pre-mRNAs and mRNAs exist in the cell.

Most hnRNPs have been found to be posttranslationally modified, suggesting that their interactions with RNAs and proteins are regulated (5). Of particular interest is the arginine methylation present in the majority of hnRNPs (26). Given the prevalence of this unusual modification in hnRNPs, it is expected to play an important role in their activity. However, the function of protein arginine methylation remains unknown.

The majority of arginine methylation in eukaryotic cells occurs within the context of RGG tripeptides (1). The arginines within these motifs are modified to $N^G N^G$ (asymmetric) dimethylarginine by type I protein methyltransferases. By compiling data on the sequence surrounding known methylated residues, an RGG motif consensus sequence was generated (21, 31). Many known type I arginine methyltransferase substrates fit the consensus (G/F)GG<u>R</u>GG(G/F), with only the underlined arginine and glycine found in all methylated sites.

Although arginine methyltransferase activity was initially detected biochemically in mammalian cell lysates, the first arginine methyltransferase gene was cloned from the yeast *Saccharomyces cerevisiae*. This type I arginine methyltransferase, termed *HMT1* for heterogeneous nuclear ribonucleoprotein methyltransferase, was identified in a screen for genes that interacted genetically with the yeast hnRNP *NPL3* (15). The same methyltransferase, alternatively called *RMT1*, was also found in a systematic search of the yeast genome for proteins containing methyltransferase motifs (6). *HMT1* is not required for normal cell viability but is synthetically lethal in at least two genetic backgrounds related to RNA maturation: in strains lacking the 80-kDa cap binding protein gene and in strains harboring the temperature-sensitive *npl3-1* allele (13, 39). The finding that human HRMT1L2/PRMT1 is a functional homolog of the product of yeast *HMT1* indicates that the cellular mechanisms involving arginine methylation are conserved throughout eukaryotes (36).

Experiments to elucidate the role of Hmt1p methylation have focused on identifying substrate proteins and examining the impact of arginine methylation on their function. HnRNP substrate proteins analyzed thus far have included four nuclear RNA binding proteins: Npl3, Hrp1/Nab4, Nab2, and Hrb1 (3, 15, 39, 41). Hrp1p and Npl3p are also structurally similar in that both share two centrally located RNA recognition motifs followed by a C-terminal RGG domain (Fig. 1A). The Npl3 protein has been shown to be involved in packaging mRNA into an export-competent mRNP (23) and might contribute to the translocation of mRNA through the nuclear complex (8, 11). The Hrp1 and Nab2 proteins are both required for efficient mRNA polyadenylation (20, 28), whereas Hrp1p plays an

* Corresponding author. Mailing address: Department of Molecular Biology, UMNDJ-SOM, 2 Medical Center Dr., Stratford, NJ 08084. Phone: (856) 566-6970. Fax: (856) 566-6291. E-mail: henrymf@umdnj.edu.
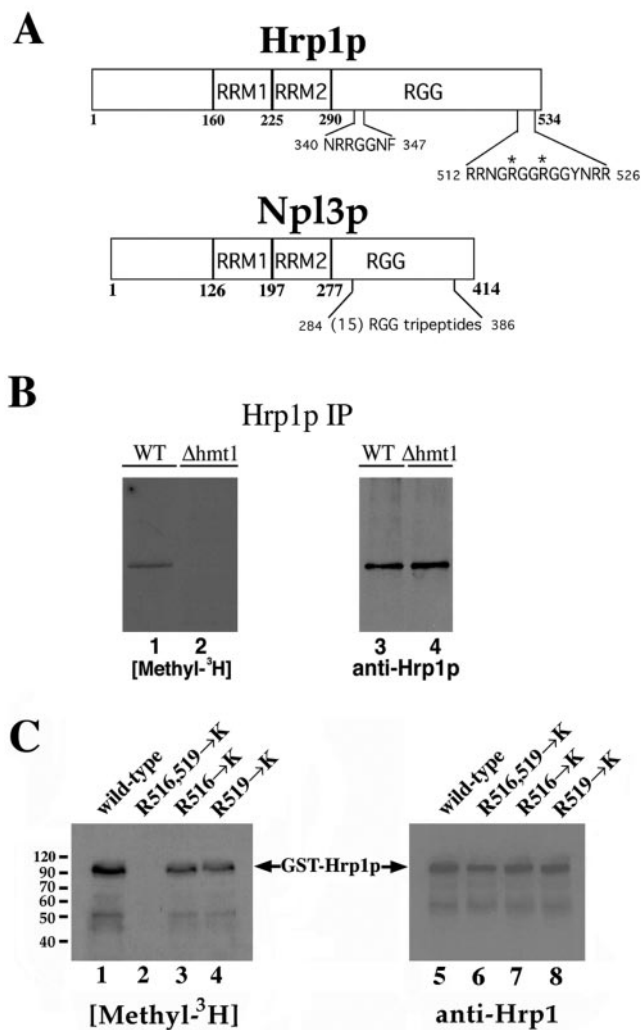
FIG. 1. Hrp1p in vitro methylation requires arginine residues at positions 516 and 519. (A) Schematic diagram of Hrp1p and Npl3p showing the location of RGG tripeptides. Each hnRNP contains two centrally located RNA recognition motifs and carboxyl-terminal repeats of the sequence RGGF/Y (3, 15). The two Hrp1p arginine residues initially tested are marked with asterisks at positions 516 and 519. (B) Hrp1p is methylated in vivo by the Hmt1/Rmt1 methyltransferase. Wild-type cells (lanes 1 and 3) and $\Delta hmt1$ cells (lanes 2 and 4) were labeled with [methyl-^{3}H]SAM as described in Materials and Methods. Immune complexes were analyzed by autoradiography (lanes 1 and 2) and Western blotting (lanes 3 and 4). (C) Methylation of GST-Hrp1 RGG→KGG mutants in vitro. E. coli extracts containing either wild-type Hrp1p (lane 1 and 5) or one of the Hrp1p mutant proteins (R516,519→K [lanes 2 and 6], R516→K [lanes 3 and 7], or R519→K [lanes 4 and 8]) were incubated with [methyl-^{3}H]SAM and recombinant Hmt1p purified from E. coli. Labeling was detected by fluorography (lanes 1 to 4) and Hrp1p expression by Western blotting (lanes 5 to 8). Relative levels of radiomethylation for the Hrp1p mutant proteins were determined by densitometry. IP, immunoprecipitation.

additional role in the nonsense-mediated decay pathway (9). In addition, all of these proteins share the ability to shuttle between the nucleus and the cytoplasm (11, 25, 38).

The first evidence for the importance of HMT1 in cellular processes was the finding that the rate of Npl3p and Hrp1p

nuclear export is decreased in strains lacking HMT1 (38). This led to the idea that one biological role for arginine methylation is in facilitating the export of certain hnRNPs from the nucleus. The mechanism by which these hnRNPs export less efficiently when not modified has not been explored.

Here we present evidence that the methylation state of one hnRNP dictates the efficient export of an mRNA-protein complex, whereas the methylation state of a second hnRNP is irrelevant for efficient export of that complex. Furthermore, we show that methylation itself is not essential for the function of this hnRNP, but rather, we conclude that the presence of unmodified RGG motifs prevents normal activity of the protein.

MATERIALS AND METHODS

Strains and media. The yeast strains used in this study are listed in Table 1. Genetic manipulations were performed essentially as described previously (32). Two different nup49-313 Δhmt1 double mutants were constructed. To create the nup49-313 Δhmt1::HIS3 double mutant (MHY285), nup49-313 was mated to strain MHY447. To create the nup49-313 Δhmt1::KanMX double mutant (MHY1078), nup49-313 was mated to strain #3171. MHY448 is a wild-type sister spore of MHY447. A previously described PCR strategy (15) was used to generate a Δhmt1::HIS3 strain (MHY499) isogenic to MHY448. An npl3-17 mutant strain (MHY1232) was created from W303a transformed with MfeI-linearized pMHY371 DNA, using the two-step pop-in/pop-out replacement method (34). A nup49-313 npl3-17 double mutant (MHY1263) expressing GFP-HRP1 was constructed by mating strain MHY1232 to strain MHY426. A nup49-313 npl3-17 double mutant (MHY1265) expressing GFP-HRP1[R516,519→K] was constructed by mating strain MHY1232 to strain MHY427. MHY1017 is a sister spore of PSY814 (13) that carries pMHY295 instead of YCpNPL3-3. Similarly, strain MHY1120 carries pMHY340. Strains MHY337 and MHY285 were transformed with pMHY337 to create strains MHY1112 and MHY1113, respectively. Strains MHY1141 and MHY1142 are pMHY339/pCGF-1C-HRP1 and pMHY339/pMHY80 double transformants of MHY1078, respectively. Strains MHY1268 and MHY1271 are pHK422 transformants of strains nup49-313 and MHY285, respectively.

Rich medium (yeast extract-peptone-dextrose [YEPD]) and synthetic defined medium supplemented with 2% of the appropriate sugar were prepared for growth of yeast (32). Liquid sporulation medium was prepared as previously described (19). Yeast strains were transformed by using the lithium acetate method (17), modified according to reference 7. Loss of URA3 plasmids from yeast cells was accomplished by plating on solid medium containing 5-fluoroorotic acid (5-FOA) (2).

Plasmid constructs. All plasmids and primers used in this study are summarized in Table 2. The Escherichia coli glutathione S-transferase (GST)-HRP1 expression vector (pGEX-HRP1) was created by ligating a 1.6-kb fragment containing the entire HRP1/NAB4 open reading frame (ORF) into pGEX-3X (Pharmacia) and has been described previously (20). Three derivatives of this plasmid (pMHY112, pMHY124, and pMHY71), harboring R516→K, R519→K, or R516,519→K mutations within HRP1, were constructed using a similar strategy. A fragment encoding both the 3′ end of HRP1 and downstream sequences was first PCR amplified from pMHY23 using primers designed to introduce both a terminal NaeI site and base substitutions at codons 516 and 519. Each PCR utilized the delR2 primer and either the delR4 (R516→K), delR3 (R519→K), or delR1 (R516,519→K) primers. Digestion of the PCR products with NaeI and HindIII yielded a 260-bp fragment that was used to replace the corresponding Eag1-HindIII wild-type fragment in pGEX-HRP1. To permit ligation with the blunt NaeI end of the PCR product, the vector EagI site was blunted with mung bean nuclease.

A yeast centromere plasmid harboring wild-type HRP1 and its flanking sequences (pMHY23) has previously been constructed (20). To generate the R→K mutant derivatives (pMHY129 [R516→K], pMHY113 [R519→K], and pMHY73 [R516,519→K]), a 1,200-bp BglII-HindIII fragment encoding the carboxyl terminus of wild-type Hrp1p was excised from pMHY23 and replaced with the corresponding mutant fragments from the E. coli GST expression vectors pMHY112, pMHY124, and pMHY71, respectively. To produce a plasmid expressing GFP-HRP1 (R516,519→K) under control of the GAL1 promoter (pMHY80), a 1,200-bp BglII-HindIII fragment encoding the carboxyl terminus of wild-type Hrp1p was excised from pCGF-1C-HRP1 and replaced with the

TABLE 1. Yeast strains used in this study

Strain	Genotype	Source or reference
W303**a**	*MAT**a** ura3-1 leu2-3,112 ade2-1 his3-11,15 trp1-1*	A. Tzagoloff
BY4741	*MAT**a** his3D1 leu2D0 met15D0 ura3D0*	Saccharomyces Deletion Project
nup49-313	*MATα Δnup49::TRP1 ura3 leu2 his3 ade2 ade3 plus pUN100-nup49-313-LEU2*	4
Y262	*MAT**a** rpb1-1 ura3-52 his4-539*	30
PSY814	*MAT**a** Δnpl3::HIS3 ura3 ade2-1 ade8 his3 leu2-3 lys1 Trp⁻ plus YCp-NPL3-3*	13
PSY818	*MATα Δhrp1::HIS3 ura3 ade2 ade8 his3 leu2 lys1 Trp⁻ plus pRS316-Hrp1*	20
#23154	*MAT**a**/MATα Δkap104::KanMX/KAP104 lys2D0/LYS2 ura3D0/ura3D0 met15D0/MET15 his3D1/his3D1 leu2D0/leu2D0*	Saccharomyces Deletion Project
#3171	*MAT**a** his3D1 leu2D0 met15D0 ura3D0 Δhmt1::KanMX*	Saccharomyces Deletion Project
MHY285	*MATα Δnup49::TRP1 Δhmt1::HIS3 ade2 ade8 leu2 his3 ura3 plus pUN100-nup49-313-LEU2*	43
MHY371	*MATα Δhrp1::HIS3 ura3 ade2 ade8 his3 leu2 lys1 Trp⁻ plus pMHY50 (CEN LEU2 MYC-HIS₆-HRP1)*	This study
MHY418	*MATα Δnup49::TRP1 ura3 leu2 his3 ade2 ade3 plus pUN100-nup49-313-LEU2 and pPS811 (2μm URA3 P_{GAL1}-GFP-NPL3)*	43
MHY419	*MATα Δnup49::TRP1 Δhmt1::HIS3 ade2 ade8 leu2 his3 ura3 plus nup49-313-LEU2 and pPS811 (2μm URA3 P_{GAL1}-GFP-NPL3)*	43
MHY424	*MAT**a** Δnup49::TRP1rpb1-1 ura3 leu2 his⁻ ade plus pUN100-nup49-313-LEU2*	This study
MHY426	*MATα Δnup49::TRP1 ura3 leu2 his3 ade2 ade3 plus pUN100-nup49-313-LEU2 and pCGF-1C-HRP1 (CEN URA3 P_{GAL1}-GFP-HRP1)*	This study
MHY427	*MATα Δnup49::TRP1 ura3 leu2 his3 ade2 ade3 plus pUN100-nup49-313-LEU2 and pMHY80 (CEN URA3 P_{GAL1}-GFP-HRP1[R516,519→K])*	This study
MHY428	*MATα Δnup49::TRP1 Δhmt1::HIS3 ade2 ade8 leu2 his3 ura3 plus pUN100-nup49-313-LEU2 and pCGF-1C-HRP1 (CEN URA3 P_{GAL1}-GFP-HRP1)*	This study
MHY429	*MATα Δnup49::TRP1 Δhmt1::HIS3 ade2 ade8 leu2 his3 ura3 plus pUN100-nup49-313-LEU2 and pMHY80 (CEN URA3 P_{GAL1}-GFP-HRP1[R516,519→K])*	This study
MHY447	*MAT**a** Δhmt1::HIS3 his3 leu2 lys1 ura3 ade2 ade8*	43
MHY448	*MAT**a** his3 leu2 lys1 ura3 ade2 ade8*	This study
MHY499	*MAT**a** Δhmt1::HIS3 his3 leu2 lys1 ura3 ade2 ade8*	This study
MHY555	*MAT**a** MYC-HIS₆-HRP1 ura3 ade2 ade8 his3 leu2 lys1*	This study
MHY570	*MATα MYC-HIS₆-HRP1[R519→K] ura3 ade2 ade8 his3 leu2 lys1*	This study
MHY571	*MATα MYC-HIS₆-HRP1[R516,519→K] ura3 ade2 ade8 his3 leu2 lys1*	This study
MHY811	*MATα MYC-HIS₆-HRP1[R516→K] ura3 ade2 ade8 his3 leu2 lys1*	This study
MHY915	*MATα Δkap104::KanMX leu2D0 ura3D0 met15D0 his3D1 plus pMHY265 (CEN URA3 KAP104-MYC)*	This study
MHY952	*MATα Δhrp1::HIS3 ura3 ade2 ade8 his3 leu2 lys1 Trp⁻ plus pMHY23 (CEN HRP1 LEU2)*	This study
MHY953	*MATα Δhrp1::HIS3 ura3 ade2 ade8 his3 leu2 lys1 Trp⁻ plus pMHY73 (CEN HRP1[R516,519→K] LEU2)*	This study
MHY954	MATα *Δhrp1::HIS3 ura3 ade2 ade8 his3 leu2 lys1 Trp⁻ plus pMHY113 (CEN HRP1[R519→K] LEU2)*	This study
MHY955	*MATα Δhrp1::HIS3 ura3 ade2 ade8 his3 leu2 lys1 Trp⁻ plus pMHY129 (CEN HRP1[R516→K] LEU2)*	This study
MHY975	*MAT**a** Δnup49::TRP1 Δhmt1::HIS3 ura3-52 ade2 ade8 leu2 plus nup49-313-LEU2 and pCGF-1C-HRP1 (CEN URA3 P_{GAL1}-GFP-HRP1)*	This study
MHY1017	*MAT**a** Δnpl3::HIS3 ade2 leu2 his3 ura3-1 lys2 plus pMHY295 (2μm URA3 NPL3)*	This study
MHY1078	*MAT**a** Δnup49::TRP1 Δhmt1::KanMX his3 leu2 ura3 lys2 ade2 ade3 plus pUN100-nup49-313-LEU2*	This study
MHY1120	*MAT**a** Δnpl3::HIS3 ade2 leu-2-3 his3 ura3 lys1 plus pMHY340 (CEN LEU2 NPL3(KGG))*	This study
MHY1112	*MATα Δnup49::TRP1 ura3 leu2 his3 ade2 ade3 plus pUN100-nup49-313-LEU2 and pMHY337 (2μm URA3 P_{GAL1}-GFP-NPL3(KGG))*	This study
MHY1113	*MATα Δnup49::TRP1 Δhmt1::HIS3 ade2 ade8 leu2 his3 ura3 plus pUN100-nup49-313-LEU2 and pMHY337 (2μm URA3 P_{GAL1}-GFP-NPL3(KGG))*	This study
MHY1141	*MAT**a** Δnup49::TRP1 Δhmt1::KanMX his3 leu2 ura3 lys2 ade2 ade3 plus pUN100-nup49-313-LEU2, pMHY339 (CEN HIS3 NPL3(KGG), and pCGF-1C-HRP1 (CEN URA3 P_{GAL1}-GFP-HRP1)*	This study
MHY1142	*MAT**a** Δnup49::TRP1 Δhmt1::KanMX his3 leu2 ura3 lys2 ade2 ade3 plus pUN100-nup49-313-LEU2, pMHY339 (CEN HIS3 NPL3(KGG)), and pMHY80 (CEN URA3 P_{GAL1}-GFP-HRP1[R516,519→K])*	This study
MHY1232	*MAT**a** npl3-17 ura3-1 leu2-3,112 ade2-1 his3-11,15 trp1-1*	This study
MHY1263	*MAT**a** npl3-17 Δnup49::TRP1 ura3 leu2-3,112 ade2 ade3 his3 trp1 leu2 his⁻ plus pUN100-nup49-313-LEU2 and pCGF-1C-HRP1 (CEN URA3 P_{GAL1}-GFP-HRP1)*	This study
MHY1265	*MAT**a** npl3-17 Δnup49::TRP1 ura3 leu2-3,112 ade2 ade3 his3 trp1 leu2 his⁻ plus pUN100-nup49-313-LEU2 and pMHY80 (CEN URA3 P_{GAL1}-GFP-HRP1[R516,519→K])*	This study
MHY1268	*MATα Δnup49::TRP1 ura3 leu2 his3 ade2 ade3 plus pUN100-nup49-313-LEU2 and pHK422 (2μm URA3 P_{GAL1}-GBP2-GFP)*	This study
MHY1271	*MAT**a** npl3-17 Δnup49::TRP1 ura3 leu2-3,112 ade2 ade3 his3 trp1 leu2 his plus pUN100-nup49-313-LEU2 and pHK422 (2μm URA3 P_{GAL1}-GBP2-GFP)*	This study

TABLE 2. Plasmids and primers used in this study

Plasmid or primer	Description	Source or reference
pRS306	Yeast integration vector *URA3*	40
pRS313	Yeast CEN cloning vector *HIS3*	40
pRS315	Yeast CEN cloning vector *LEU2*	40
pGEX-HRP1	Hrp1 fused to the carboxyl terminus of GST in the pGEX-3X vector	20
pCCF-1A	2μm *URA3* GFP-*HRP1* under GAL1 promoter	18
pCGF-1C-HRP1	2μm *URA3* GFP-*HRP1* under GAL1 promoter	20
HRP1(492-534)-p12-2×GFP2	2μm *URA3* vector carrying a C-terminal HRP1 peptide fused the mutant p12 nes followed by two GFPs	24
pHK422	2μm *URA3* GBP2-GFP under *GAL1* promoter	42
YEp352	Yeast 2μm cloning vector *URA3*	16
pPS811	2μm *URA3* GFP-*NPL3* under *GAL1* promoter	25
pMHY23	*CEN LEU2* vector carrying a 2.2-kb chromosomal fragment encoding *HRP1*	20
pMHY40	*CEN URA3* vector carrying a 5.2-kb chromosomal fragment encoding *HRP1*	13
pMHY47	*CEN LEU2* vector carrying NcoI-*HRP1*	This study
pMHY48	*CEN LEU2* vector carrying His$_6$-*HRP1*	This study
pMHY50	*CEN LEU2* vector carrying Myc-His$_6$-*HRP1*	This study
pMHY67	*URA3* yeast integration vector carrying Myc-His$_6$-*HRP1*	This study
pMHY71	GST-*HRP1* with a R516,519→K substitution	This study
pMHY73	*CEN LEU2* vector carrying *HRP1* with R516,519→K substitution	This study
pMHY80	2μm *URA3* vector carrying *GFP-HRP1*(R516,519→K) under GAL1 promoter control	This study
pMHY112	*GST-HRP1*(R519→K)	This study
pMHY113	*CEN LEU2* vector carrying *HRP1*(R519→K)	This study
pMHY114	*CEN LEU2* vector carrying Myc-His$_6$-*HRP1* (R519→K)	This study
pMHY120	*URA3* yeast integration vector carrying Myc-His$_6$-*HRP1*(R519→K)	This study
pMHY124	GST-*HRP1*(R516→K)	This study
pMHY129	*CEN LEU2* vector carrying *HRP1*(R516→K)	This study
pMHY132	*CEN LEU2* vector carrying Myc-His$_6$-*HRP1* (R516,519→K)	This study
pMHY133	*CEN LEU2* vector carrying Myc-His$_6$-*HRP1* (R516→K)	This study
pMHY137	*URA3* yeast integration vector carrying Myc-His$_6$-*HRP1* (R516→K)	This study
pMHY138	*URA3* yeast integration vector carrying Myc-His$_6$-*HRP1* (R516,519→K)	This study
pMHY292	*CEN HIS3* vector carrying *NPL3*	This study
pMHY295	2μm *URA3* vector carrying *NPL3*	This study
pMHY296	2.5-kb SphI-SmaI fragment carrying *npl3-17* in YEp352	This study
pMHY313	*CEN HIS3* vector carrying *npl3-17*	This study
pMHY334	2μm *URA3* vector carrying a C-terminal HRP1 (R516,519→K) peptide fused to the mutant p12 nes followed by two GFPs	This study
pMHY337	2μm *URA3* GAL1 promoter expression vector carrying *NPL3*(KGG)-GFP	This study
pMHY339	*CEN HIS3* vector carrying *NPL3*(KGG)	This study
pMHY340	*CEN LEU2* vector carrying *NPL3*(KGG)	This study
pMHY341	GST-*HRP1* with a R516,519→E substitution	This study
pMHY342	GST-*HRP1* with a R516,519→Q substitution	This study
pMHY343	*CEN LEU2* vector carrying *HRP1* with a R516,519→E substitution	This study
pMHY344	*CEN LEU2* vector carrying *HRP1* with a R516,519→Q substitution	This study
pMHY345	2μm *URA3* vector carrying a C-terminal HRP1 (R516,519E) peptide (392-534) fused to a mutant p12 nes followed by two GFPs	This study
pMHY346	2μm *URA3* vector carrying a C-terminal HRP1 (R516,519Q) peptide (392-534) fused to a mutant p12 nes followed by two GFPs	This study
pMHY351	2μm *URA3* vector carrying a C-terminal *HRP1* (R516,519K) peptide (492-534) fused to a mutant p12 nes followed by two GFPs	This study
pMHY352	2μm *URA3* vector carrying a C-terminal HRP1 (R516,519E) peptide (492-534) fused to a mutant p12 nes followed by two GFPs	This study
pMHY353	2μm *URA3* vector carrying a C-terminal HRP1 (R516,519Q) peptide (492-534) fused to a mutant p12 nes followed by two GFPs	This study
pMHY371	*URA3* yeast integration vector carrying *npl3-17*	This study
#293	5′-CTTCGGATCCTGAACGGCCTCGCGTTTGTTGAATTTG-3′	
#294	5′-GGAGGATTGTCATCTCTTTCAACAGTAGTGA-3′	
delR1	5′-CTCACAAGCCGGCAAAGGTGGTAAAGGTGGATACAATAGACG-3′	
delR2	5′-AGCTATGACCATGATTACGCC-3′	
delR3	5′-CTCACAAGCCGGCCGTGGTGGCAAAGGTGGATACAATAGACG-3′	
delR4	5′-CTCACCAGCCGGCAAAGGTCGTCGCGGTGGATACAATAGACG-3′	
Hrp1(930-951)	5′-CGCAAGATCGAAATCAAGAGAGC-3′	
Hrp1(138-166)	5′-GCTTGTGATTATACATTCTAGCATAGTG-3′	
HRP1(NcoI)	5′-AGAGCTCCCCATGGCTTATTTAACTTATTCTCTATTTTCTCAGACTT-3′	
HRP1(26 mer)	5′-CTTCCGCTCTCTCCTTTCCGCCACTG-3′	
Nco-Myc-upper	5′-CATGGAGCAGAAGCTGATTAGCGAGGAAGATCTGAA-3′	
Nco-Myc-lower	5′-CATGTTCAGATCTTCCTCGCTAATCAGCTTCTGCTC-3′	

TABLE 2—*Continued*

Plasmid or primer	Description	Source or reference
NPL3 #1	5′-CAATCCTCCACCAATCAGAAGATCAAATAAAGGTGGCTTCAGAGGTAA AGGCGGCTTCAAAGGCGGCTTCAAAGGTGGCTTCAAAGGCGGTTTCTC GAGTTCCG-3′	
NPL3 #2	5′-CTAGCGGAACTCGAGAAACCGCCTTTGAAGCCACCTTTGAAGCCGCCTT TGAAGCCGCCTTTACCTCTGAAGCCACCTTTATTTGATCTTCTGATTGGT GGAGGATTG-3′	
NPL3 #3	5′-TCGAAAGGCGGCTTCGGTGGCCCAAAAGGTGGATTTGGTGGTCCAAAA GGTGGTTACGGTGGCTATTCCAAAGGTGGCTACGGTGGCTATT-3′	
NPL3 #4	5′-CGAATAGCCACCGTAGCCACCTTTGGAATAGCCACCGTAACCACCTTTT GGACCACCAAATCCACCTTTTGGGCCACCGAAGCCGCCTT-3′	
NPL3 #5	5′-CGAAAGGCGGATATGGTGGCTCCAAAGGTGGTTACGATAGTCCTAAAG GTGGTTACGATAGTCCAAAAGGTGGTTATTCCAAAGGTGGCTATGGTG GTCCAAGAAATGATTACGGTCCTC-3′	
NPL3 #6	5′-CTAGGAGGACCGTAATCATTTCTTGGACCACCATAGCCACCTTTGGAAT AACCACCTTTTGGACTATCGTAACCACCTTTAGGACTATCGTAACCACCT TTGGAGCCACCATATCCGCCTTT-3′	
NPL3 #7	5′-CTAGCTACCTAGGGGTAGCTACGGTGGTTCAAAAGGTGGTTATGATGG TCCAAGAGGCGATTATGGTCCTCCAAGAGATGCATACAGAACCAGAGA TGCTCCACGTGAAAGATCACCAA-3′	
NPL3 #8	5′-CCTGGTTGGTGATCTTTCACGTGGAGCATCTCTGGTTCTGTATGCATCT CTTGGAGGACCATAATCGCCTCTTGGACCATCATAACCACCTTTTGAAC CACCGTAGCTACCCCTAGGTAG-3′	
HRP1 R to E	5′-CTCACAAGCCGGCGAAGGAGGAGAAGGTGGATACAATAGACGTAATA ATGGC-3′	
HRP1 R to Q	5′-CTCACAAGCCGGCCAAGGTGGCCAAGGTGGATACAATAGACGTAATAA TGGC-3′	
Hrp1 492/534	5′-CTCCAAGCTTATGGGTGGATCCGGTGATCGTGATCGTAAC-3′	
Hrp1 534/492	5′-CTTGTGGCCGTTTACGTC-3′	
HRP1(EcoR1)	5′-CATTGAATTCCCTATTATATGGATGGTAGCC-3′	
HRP1(1267)	5′-ACCAACCACAGCAAGATTC-3′	

corresponding mutant fragment from pMHY73. The construction of a yeast vector encoding Hrp1p tagged at the amino terminus with six histidines and the 9E10 c-Myc epitope (pMHY50) required several steps. First, an NcoI site was introduced at the ATG codon of the *HRP1* ORF by ligating a SpeI-SacI PCR product encoding *HRP1* upstream sequences (from pMHY40, *CEN URA3 HRP1*) and a SacI-HindIII restriction fragment (from pMHY23, *CEN LEU2 HRP*) encoding the *HRP1* ORF and downstream sequences at a common SacI site and inserting them into the SpeI/HindIII sites of pMHY14 (*CEN LEU2*) to yield pMHY47. The primers used were HRP1(NcoI) and HRP1(26-mer). Second, pMHY48 (*CEN LEU2* His₆-*HRP1*) was generated by swapping a NcoI-BglII fragment from plasmid pMHY47 with a NcoI-BglII fragment from pET-15b-HRP1 (20). Finally, pMHY50 (*CEN LEU2* Myc-His₆-*HRP1*) was constructed by inserting two annealed oligonucleotides (Nco-Myc-upper and Nco-Myc-lower) encoding the 9E10 c-Myc epitope into the NcoI site of pMHY48. To produce a Myc-His₆-*HRP1* R→K mutant derivatives plasmid, an AatII-HindIII fragment encoding the mutant carboxyl terminus of *HRP1* from plasmids pMHY124 (R516→K), pMHY113 (R519→K), and pMHY71 (R516,519→K) was used to replace the corresponding wild-type fragment in plasmid pMHY50, yielding plasmids pHMY133, pMHY114, and pMHY132, respectively. To construct the Myc-His₆-*HRP1* genomic integration plasmid (pMHY67), a 2.2-kb SpeI-HindIII fragment from pMHY50 was inserted into the SpeI-HindIII site of pRS306. HindIII-NotI restriction fragments encoding the mutant *HRP1* alleles were excised from pMHY133, pMHY114, and pMHY132 and ligated into pRS306 to yield the integration vectors pMHY137, pMHY120, and pMHY138, respectively.

Plasmids pMHY341 [*GST-HRP1* R516,519(E)] and pMHY342 [*GST-HRP1* R516,519(Q)] were constructed by using the same strategy as for pMHY71 except that the 5′ primers HRP1 R to E and HRP1 R to Q, respectively, replaced primer delR1. Plasmids pMHY343 [*HRP1* R516,519(E)] and pMHY344 [*HRP1* R516,519(Q)] were generated by replacing a BglII-HindIII fragment of wild-type *HRP1* (pMHY23) with corresponding mutant fragments from pMHY341 and pMHY342, respectively. An AatII-EcoRI fragment from plasmid HRP1 [(392-534)-2xGFP] was swapped with the corresponding mutant PCR products from pMHY73, pMHY341, and pMHY342 to generate the respective R→K, R→E, and R→Q derivative plasmids. In all cases, the HRP1(1267) and HRP1(EcoR1) primer set was used. Plasmids pMHY350, pMHY351, pMHY352, and pMHY353

were constructed by replacing the HindIII-EcoRI fragments with same enzyme-digested PCR products from HRP1 (392-534)-2xGFP, pMHY334, pMHY345, and pMHY346, respectively. In all cases, the combination of the Hrp1 492/534 primer and the Hrp1 534/492 primer was used. Compared to their parent plasmids, these four plasmids contain a shorter C-terminal Hrp1 peptide (amino acid residues 492 to 534).

A yeast centromere *HIS3* plasmid harboring wild-type *NPL3* and its flanking sequences (pMHY292) was created by inserting a 2.5-kb AclI-EcoRV chromosomal fragment encoding *NPL3* into the ClaI-EcoRV sites of pRS313. A 2μm *URA3 NPL3* plasmid (pMHY295) was generated by subcloning a 2.5-kb SalI-SmaI *NPL3* fragment into YEP352. An *npl3-17* version of this plasmid (pMHY296) was created by first amplifying a 357-bp fragment of *NPL3* from pMHY295 using the mutagenic primers #293 and #294. The resulting PCR product, harboring the *npl3-17* point mutations, was digested with BamHI/BsaBI and used to replace the corresponding wild-type BglII/BsaBI *NPL3* fragment in pMHY295. An *npl3-17* integration plasmid (pMHY371) was made by inserting a SalI-SmaI fragment carrying *npl3-17* from pMHY296 into pRS306. The construction of a yeast vector encoding GFP-NPL3 (RGG→KGG) under *GAL1* control (pMHY337) required two steps. First, a BsaB1/SexA1 fragment encoding a carboxyl-terminal portion of wild-type Npl3p was excised from pPS811 and replaced with two sets of annealed oligonucleotides (NPL3 #1 and NPL3 #2; NPL3 #7 and NPL3 #8) to yield pMHY336. Next, two additional sets of annealed oligonucleotides (NPL3 #3 and NPL3 #4; NPL3 #5 and NPL3 #6) were simultaneously ligated into pMHY336 digested with AvrII and XhoI to generate pMHY337. To generate a *CEN HIS3* vector encoding the *NPL3* (RGG→KGG) gene under control of its own promoter (pMHY339), a 1.2-kb AlwNI-SexA1 fragment encoding the C terminus of *NPL3* (RGG→KGG) was excised from pMHY337 and used to replace the corresponding wild-type fragment of pMHY292. A *CEN LEU2* version (pMHY340) was produced by inserting a BamHI-SalI fragment encoding *NPL3* (RGG→KGG) from pMHY339 into pRS315.

Chromosomal integration of recombinant *hrp1* alleles. The pop-in/pop-out method, developed by Scherer and Davis (34), was used to replace the wild-type *HRP1* chromosomal allele with the plasmid-borne *hrp1* variants. Briefly, each *URA3*-based integrating plasmid was linearized with MfeI and transformed into

strain MHY370 [Δ*hrp1*::*HIS3* plus pMHY23 (CEN *LEU2 HRP1*)], and potential integrants were selected by growth on Ura⁻ drop-out plates. Potential integrants were grown in the presence of leucine for 30 generations, and those cells cured of pMHY23 (*CEN LEU2 HRP1*) were identified by comparative growth on SC plates lacking uracil or both uracil and leucine. Finally, excision of the plasmid is counterselected by streaking Leu⁻ colonies onto 5-FOA. Subsequent loss of the His⁺ phenotype suggests replacement of the Δ*hrp1*::*HIS3* allele with the mutant *hrp1* allele. PCR amplification followed by restriction analysis and DNA sequencing was used to confirm the Hrp1 R→K changes. Chromosomal DNA from each of the six integrants was isolated using the method described by Rose and Hieter (32) and purified using the Qiaquick kit (QIAGEN, Inc.). The 3′ terminus of *HRP1*, encoding the RGG domain, was PCR amplified using the primers Hrp1 (930–951) and Hrp1 (138–166). Arg→Lys changes were detected by digesting the resulting products (~800 bp) with either EagI or BglI. The R_{516}→K and $R_{516,519}$→K changes were identified by loss of an EagI site, whereas the R_{519}→K change was detected by the presence of a BglI site. DNA sequencing of the PCR products confirmed the nucleotide changes (Davis Sequencing).

In vitro methylation reaction. Recombinant Hmt1p (0.2 μg) expressed and purified from *E. coli* (15) was incubated with 7 μl of *S*-adenosyl-L-[*methyl*-³H]methionine (³H-SAM) (specific activity of 84 mCi/mmol; Amersham Biosciences) and 20 μg of *E. coli* whole cell extracts (expressing either wild-type or R→K Hrp1p mutants) in a 15-μl volume of methylation assay buffer. Reaction conditions and sample analysis have been described previously (15).

In vivo methylation and immunoprecipitation. Cells were grown to 10⁶ cells/ml at 30°C in 75 ml of synthetic defined medium supplemented with the required amino acids and 2% glucose. Labeling was initiated by the addition of 100 μCi of ³H-SAM (specific activity of 84 mCi/mmol; Amersham Biosciences), and incubation was continued until a level of 10⁷ cells/ml was reached. The labeled cells were pelleted, washed once in lysis buffer (50 mM Tris-HCl [pH 7.5], 100 mM NaCl, 5 mM EDTA, 10% glycerol, 1% Triton X-100), and resuspended in 400 μl of lysis buffer supplemented with protease inhibitors (10 mg of phenylmethylsulfonyl fluoride/ml and 2.5 μg [final] each of aprotinin, leupeptin, chymostatin, and pepstatin/ml) and 1 M dithiothreitol. Cells were lysed by the addition of 300 μg of glass beads (Biospec Products) and continuous vortexing for 10 min at 4°C. Protein extracts were clarified by a 10-min centrifugation at 13,000 rpm in an Eppendorf 5415C centrifuge at 4°C, and the protein concentration was determined by using a Bio-Rad protein assay kit. Lysates were precleared by a 1-h incubation with a combination of 10 μl of Sepharose CL-4B beaded agarose (Sigma) and 10 μl of protein A-Sepharose (Amersham Biosciences) at 4°C. Myc-His₆-Hrp1p-antibody complexes were precipitated by addition of affinity-purified anti-Hrp1p antibody immobilized on protein A-Sepharose (5 μl of a 50% slurry) to the precleared lysate, followed by incubation for 1 h with rocking at 4°C. Conversely, Myc-Kap104-antibody complexes were precipitated by addition of a c-Myc (9E10) antibody–agarose conjugate (10 μl of a 50% slurry; Santa Cruz Biotechnology). Beads were washed three times with lysis buffer, and immunoprecipitated proteins were resolved by sodium dodecyl sulfate-polyacrylamide gel electrophoresis (SDS-PAGE) and visualized by Coomassie staining. Following staining, the gel was soaked in EN³HANCE autoradiography enhancer (NEN Life Sciences) as directed by the manufacturer. Dried gels were exposed to preflashed HyperFilm (Amersham Biosciences) at −80°C for 1 to 14 days.

Immunoblot analysis. Total cell extracts were prepared (3) from cells grown in either YEPD or drop-out medium. Proteins were resolved by SDS-PAGE, transferred, and immunoblotted as described previously (3). Rabbit anti-Hrp1p (14), anti-Npl3p (3, 10), and anti-Yrb1p (35) were used at 1:5,000. Mouse monoclonal anti-Myc (9E10) (Santa Cruz Biotechnology) was used at 1:1,000. The blots were then incubated with horseradish peroxidase (HRP)-conjugated antibodies (antimouse or antirabbit) at a concentration of 1:5,000 and detected with ECL Western blotting reagents (Amersham Biosciences).

Export assay. The nuclear export assay was performed exactly as described previously (25). Briefly, cells containing various reporter plasmids are induced for 2 h in medium containing galactose to express the reporter followed by repression for 2 h in YEPD. Cells are then incubated at either 25°C or 36°C for 5 h and examined for green fluorescent protein (GFP) fluorescence.

Indirect immunofluorescence. Indirect immunofluorescence microscopy was performed as previously described (33). Affinity-purified rabbit anti-Npl3p (3) and anti-Hrp1p (14) were used at 1:1,000. The 4′, 6-diamidino-2-phenylindole (DAPI) nuclear stain was used at 1:1,000.

UV cross-linking of Npl3 and Hrp1p to poly(A)⁺ RNA. Isolation of UV-linked poly(A)⁺ RNA-ribonucleoprotein (RNP) complexes and analysis of cross-linked Npl3p and Hrp1p by SDS-PAGE and Western blotting were done essentially as described previously (23). A 500-ml culture of both a wild-type (MHY448) and Δ*hmt1* (MHY499) strain was grown to an optical density at 600 nm of 1.0. Cells were harvested and washed twice with phosphate-buffered saline, and each culture was split into two equal portions. The first portion was not UV irradiated, whereas the second portion was UV irradiated for three times for 2.5 min each on ice in the Stratalinker 1800 (Stratagene). All samples were washed in phosphate-buffered saline and lysed in lysis buffer. The poly(A)⁺ RNA was purified and the proteins were analyzed as described previously (23). All eluate samples were loaded normalized to the purified RNA, and 10 optical density at 260 nm units were loaded per lane.

Immunoprecipitation. Cells were grown at 30°C to a density of 10⁷ cells/ml in 250 ml of YEPD. Cells were then pelleted, washed once in lysis buffer (50 mM Tris-HCl [pH 7.5], 100 mM NaCl, 5 mM EDTA, 10% glycerol, 1% Triton X-100), and resuspended in 1,200 μl of lysis buffer. Protease inhibitors were added to a final concentration of 0.1 μg/ml each of antipain, aprotinin, chymostatin, leupeptin, and pepstatin. The cells were split into four microfuge tubes, glass beads were added, and the cells were lysed by vortexing for 8 min (2-min intervals) at 4°C. After a 10-min microfuge spin, the clarified supernatants were precleared for 1 h with 20 μl of protein A-agarose beads at 4°C with gentle agitation. The extract was again cleared and incubated with 20 μl of agarose conjugated to affinity-purified polyclonal anti-Hrp1 antibody for 2 h. The anti-Hrp1p agarose beads were then washed three times with lysis buffer (1 ml) by repeated low-speed centrifugation. When required, RNase A was added as described for Fig. 6A.

RESULTS

Hrp1p is arginine methylated in vivo by Hmt1p/Rmt1p. To elucidate the role of arginine methylation in nuclear export, we first examined the Hrp1p shuttling protein of budding yeast. Although we have previously shown that Hrp1p is an efficient substrate for the *HMT1/RMT1* arginine methyltransferase in vitro (38), this result has not been confirmed in vivo. To demonstrate that Hrp1p was methylated in living cells, we employed an in vivo arginine methylation assay we developed to monitor the methylation of several nucleolar proteins (43). This assay is based on the ability of the methyl donor *S*-adenosyl-L-methionine (SAM) to be efficiently transported across the plasma membrane of yeast. The transferable methyl group on SAM is tritium labeled to permit detection of methylated proteins. Both wild-type and Δ*hmt1* mutant yeast cells were labeled with [³H]SAM, and proteins were examined by gel electrophoresis and fluorography. In this assay, substrates of the Hmt1 methyltransferase are recognized as radiolabeled proteins present only in the wild-type extract (43).

A radiolabeled protein of the size expected for Hrp1p was not apparent in whole-cell extracts (data not shown). However, precipitation with anti-Hrp1p antibodies specifically concentrated a radiolabeled protein of the correct size (Fig. 1B, lane 1). This band was absent in the Δ*hmt1* extract, indicating that the methyltransferase is required for the labeling (Fig. 1B, lane 2). Immunoblot experiments confirmed that equivalent levels of this protein precipitated from both extracts and was in fact Hrp1p (Fig. 1B, lanes 3 and 4). These results demonstrate that Hmt1p is required for Hrp1p methylation in vivo.

In vitro methylation of Hrp1 by Hmt1p requires R516 and R519. Since dimethylated arginine residues are frequently found in the context of RGG tripeptides, arginine residues at positions 516 and 519 represented two likely methylation sites (Fig. 1A). Although lysine and arginine residues are similar in structure and chemical properties, synthetic peptides harboring KGG tripeptides are not substrates for methylation in vitro (29). Therefore, to test the possibility that Hmt1p methylates one or both of these sites, recombinant GST-Hrp1 protein containing arginine-to-lysine changes was constructed and ex-
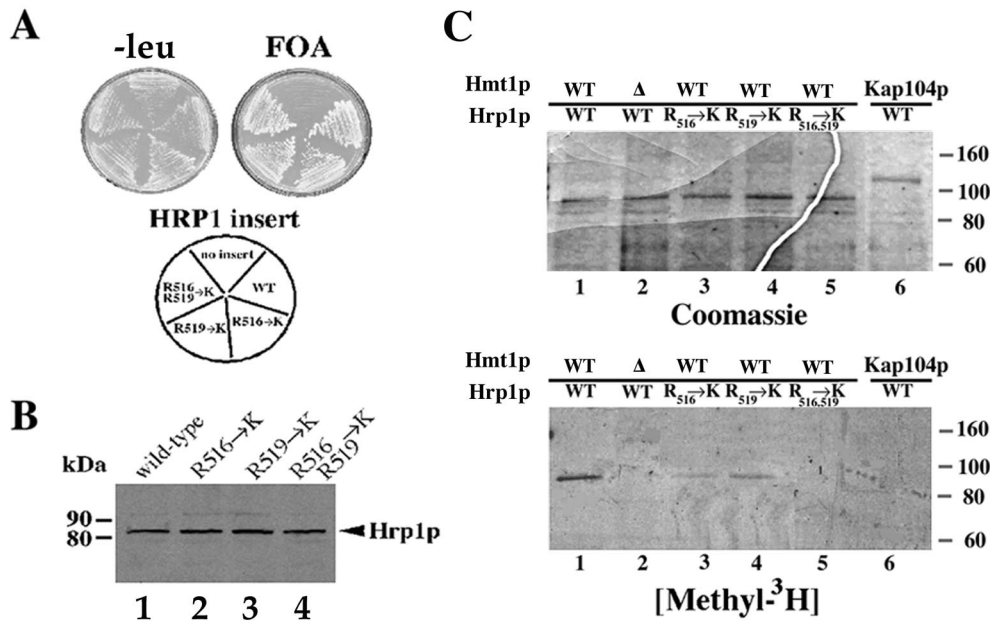
FIG. 2. In vivo methylation of Hrp1 by Hmt1p requires R516 and R 519. (A) *HRP1* R→K mutant alleles rescue the Δ*hrp1* lethal phenotype. Δ*hrp1* cells bearing a *CEN URA3 HRP1* plasmid (PSY818) and transformed with a *CEN LEU2* vector carrying either a wild-type (pMHY23) (WT), R516→K (pMHY129), R519→K (pMHY113), or R516,519→K (pMHY73) *hrp1* allele are shown. Transformants were streaked on synthetic complete medium lacking leucine (left) or containing 5-FOA (right). A plate schematic (lower) indicates the *HRP1* allele carried by each plasmid. (B) Wild-type Hrp1 and RGG→KGG mutant proteins are expressed at equal levels. Yeast lysates prepared from Δ*hrp1* cells covered with a plasmid expressing either wild-type Hrp1p (pMHY23; lane 1) or one of three Hrp1p mutant proteins (R516→K [pMHY129; lane 2], R519→K [pMHY113; lane 3], or R516,519→K [pMHY73; lane 4]), were separated by SDS-PAGE and analyzed by Western blotting with antibodies against Hrp1p. (C) In vivo methylation of Hrp1 by Hmt1p requires R516 and R519. Wild-type (lane 1) (WT) and Δ*hmt1* (lane 2) (Δ) cells carrying an integrated Myc-His$_6$-HRP1 allele were grown in parallel with wild-type cells integrated with the mutant R516→K (lane 3), R519→K (lane 4), or R516,519→K (lane 5) *HRP1* allele. Radiomethylated protein immunopurified from cell extracts with anti-Hrp1p-conjugated Sepharose beads was subjected to SDS-PAGE. To control for translational label incorporation, Kap104-Myc protein (Kap104p) was immunopurified in parallel (lane 6). Proteins were Coomassie stained, and labeling was detected by fluorography. Strains MHY555, MHY570, MHY571, MHY811, and MHY915 were examined.

pressed in *E. coli*, which lacks arginine methyltransferase activity (26).

E. coli extracts containing the different GST-Hrp1p proteins were incubated with the radiolabeled methyl donor ^{3}H-SAM in the presence of purified GST-Hmt1 enzyme (Fig. 1C, lanes 1 to 4). Strikingly, Hmt1p is completely unable to methylate Hrp1p having lysine residues at positions 516 and 519 (Fig. 1C, lane 2). Furthermore, Hrp1p radiolabeling in single point mutants (R516→K and R519→K) was reduced to approximately 50% of that observed for wild-type Hrp1p (Fig. 1C, lanes 3 and 4). Western blot analysis of the methylated *E. coli* extracts using anti-Hrp1p antibodies revealed that equal amounts of Hrp1 were present (Fig. 1C, lanes 5 to 8). Thus, arginine residues at positions 516 and 519 are essential for methylation of Hrp1p by Hmt1p in vitro. By this assay, a third RGG tripeptide at position 342 (Fig. 1A) is not a substrate for Hmt1p (unpublished result). These results also confirm that lysine residues are not substrates for Hmt1-dependent methylation in the context of a whole protein.

Hrp1p R→K mutants are functional and present at wild-type levels. Previous work has shown that although Hrp1 is required for cell viability, the Hmt1 methyltransferase is dispensable for normal cell growth (13, 15). Given that we have now established that Hmt1p is also responsible for Hrp1p methylation in living cells, the loss of Hrp1p methylation is not

predicted to dramatically impact cell viability under standard lab growth conditions. However, the functional consequences of converting RGG tripeptides within Hrp1p to KGG are unknown.

To address this issue, we compared the growth of wild-type cells to that of those expressing Hrp1p (RGG→KGG) mutants. Both single and double Hrp1 (RGG→KGG) proteins are functional, in that the mutants rescue the lethal *hrp1* null allele (Fig. 2A). These mutant cells are neither cold sensitive (15°C) nor temperature sensitive (36°C) (unpublished results). Furthermore, the growth of cells on plates at 30°C expressing the *hrp1* (RGG→KGG) alleles was indistinguishable from that of those with a wild-type allele (Fig. 2A). Consistent with these observations, both wild-type and mutant Hrp1p are expressed at equivalent levels in these cells as determined by immunoblot analysis using anti-Hrp1 antibody (Fig. 2B).

In vivo methylation of Hrp1 by Hmt1p requires R516 and R519. To determine whether *HMT1* is also required to methylate R516 and R519 in vivo, we employed the in vivo methylation assay. The ^{3}H-SAM-labeled cells carried either an epitope-tagged *HRP1* allele (Myc-His$_6$-HRP1) or one of the epitope-tagged R→K alleles that had replaced the wild-type chromosomal *HRP1* allele (see Materials and Methods). All tagged alleles are functional in that cell viability is retained following replacement of wild-type *HRP1* (our unpublished

results). Myc-His$_6$-*HRP1* was immunopurified from extracts made from each culture, and methylation levels were visualized after gel electrophoresis by fluorography. Coomassie protein staining revealed that similar amounts of Hrp1p were immunoprecipitated from the extracts (Fig. 2C, lanes 1 to 5). These values were used to standardize Hrp1p methylation levels. In strains expressing Hrp1 (R516→K) or Hrp1 (R519→K), Hrp1 radiolabeling was reduced to approximately 10% of that observed for the isogenic parent strain (Fig. 2C, compare lane 1 to lanes 3 and 4). This result suggests that the loss of either R516 or R519 within Hrp1p results in reduced methylation of the remaining arginine residue. Moreover, Hrp1p methylation was not detected in cells lacking Hmt1p or expressing the Hrp1p (R516/519→K) double mutant (Fig. 2C, lanes 2 and 5). The inactivity of Hrp1p (R516/519→K) as an Hmt1p substrate cannot be explained by gross misfolding of the Hrp1 protein because, as we have shown, the mutant protein is functional. The absence of Hrp1p (R516/519→K) radiolabeling also suggests that tritium incorporation is due to methylation and not translation. Accordingly, Kap104, a protein similar in size and abundance to Hrp1p but lacking potential methylation sites, is also not radiolabeled in this assay (Fig. 2C, lane 6). Thus, the two arginines present within the carboxyl-terminal RGG domain of Hrp1p are essential for methylation by Hmt1p in vivo.

Hrp1p R→K mutants properly localize to the nucleus. The steady-state localization of Hrp1p is predominately nuclear in both wild-type and Δ*hmt1* cells (13). A carboxyl-terminal Hrp1p peptide (43 amino acids) harboring two RGG peptides was found to mediate the nuclear import of a GFP fusion protein (24). This nuclear localization signal (NLS) was designated an rg-NLS to distinguish it from the basic cNLSs (24). Since both Hrp1p methylarginines are located within these two RGG tripeptides, it was important to determine whether R→K substitutions would affect nuclear localization. In Δ*hrp1* cells containing either plasmid-borne *HRP1* or *hrp1* (R→K) alleles, Hrp1p is located in the nucleus, as judged by immunofluorescence (Fig. 3A, center panels) and coincident with the nuclear DAPI stain (Fig. 3A, right panels). These results demonstrate that conserved arginine-to-lysine substitutions within the two methylated RGG tripeptides do not impact the nuclear localization of Hrp1p under standard growth conditions.

To confirm that a carboxy-terminal Hrp1p peptide harboring KGG sequences was sufficient for nuclear import, the mutant protein sequences were tagged with a tandem repeat of two GFPs (2xGFPs) and visualized in living cells (Fig. 3B). Although 2xGFP alone localized to the cytoplasm, both wild-type RGG and mutant KGG Hrp1p peptides targeted the GFP fusion to the nucleus (Fig. 3B). This localization was abolished by substitution with either a neutral (glutamine) or negatively charged (glutamate) amino acid (Fig. 3B). These results demonstrate that both RGG- and KGG-rich domains act as functional NLSs in vivo. However, nonconserved changes to either glutamine or glutamate disrupt the import signal.

Hrp1 (R516/519→K) nuclear export requires cellular HMT1 expression. To determine whether Hrp1p lacking arginine-methylated residues can exit the nucleus in a wild-type *HMT1* strain, we employed a nuclear export assay (25). This assay exploits the properties of a thermosensitive nucleoporin mutant *nup49-313* strain (4). At the restrictive temperature, import into the nucleus is blocked, whereas export out of the

nucleus is unaffected in this mutant (25). In our experiment, plasmids encoding GFP fusions of either the Hrp1 protein or the Hrp1 (R516/519→K) protein under control of the *GAL1* promoter were transformed into a *nup49-313* strain and a *nup49-313* Δ*hmt1* double-mutant strain. Both GFP-Hrp1 fusion proteins properly localized to the nucleus at 25°C and were functional, in that they rescued the *hrp1* null allele (our unpublished data). If the GFP-Hrp1 fusion proteins shuttle, they should accumulate in the cytoplasm of *nup49-313* cells after a shift to 36°C.

Consistent with our previous studies (20, 38), GFP-Hrp1p accumulated in the cytoplasm of *nup49-313* cells after a shift to 36°C but failed to leave the nucleus in the *nup49-313* Δ*hmt1* strain, indicating that the nuclear export of Hrp1p is affected by cellular methylation (Fig. 3C, panels D and L). Importantly, the same distribution patterns were observed for the GFP-Hrp1 (R516/519→K) fusion protein after a shift to 36°C (Fig. 3C, panels H and P). Thus, unmodified Hrp1p is exported from the nucleus in wild-type cells but not in a strain lacking *HMT1*. Taken together, our data support a model in which Hrp1p export requires cellular arginine methyltransferase activity whereas the methylation of Hrp1p itself is dispensable.

Npl3 (R→K) nuclear export is independent of cellular arginine methylation. To explain how Hrp1 (R516/519→K) is actively exported in wild-type *HMT1* cells but retained in the nucleus of Δ*hmt1* cells, we reasoned that the export defect observed in the mutant cells might be indirectly due to another arginine-methylated protein required for proper RNP complex formation and/or export. In pre-mRNA processing, some hnRNP proteins dissociate from the maturing transcript in the nucleus, whereas others remain associated with the transcript to form an RNP complex that is exported to the cytoplasm. Hrp1p belongs to the latter class of hnRNPs, which remains RNP associated and shuttle between the nucleus and the cytoplasm. Another member of this class, Npl3p, is a likely candidate to mediate Hrp1p/RNP complex export in a methylarginine-dependent manner.

In order to test whether Npl3p methylation is required for export of an RNP complex containing Hrp1p, we generated a yeast strain expressing a mutant Npl3 protein in which all 15 RGG tripeptides were converted to KGG (see Materials and Methods). To verify that the Npl3p (KGG) mutant was no longer methylated, we performed an in vivo methylation assay. Wild-type yeast cells expressing either Npl3p or Npl3p (KGG) were labeled with ^{3}H-SAM, and whole cell extracts were resolved by gel electrophoresis (Fig. 4A). The Npl3p protein migrates at 58 kDa on these gels (Fig. 4A, lane 1), and its labeling is Hmt1p dependent (43). Significantly, the Npl3p (KGG) mutant is not methylated in cells expressing a functional arginine methyltransferase (Fig. 4A, lane 2). Immunoblot experiments confirmed that equivalent levels of Npl3p are present in both extracts (Fig. 4A, lanes 3 and 4). Using the same approaches described for the Hrp1 (R→K) mutants, we determined that the Npl3 (KGG) mutant protein was present at levels equal to wild-type levels (Fig. 4A), localized to the nucleus (Fig. 4B), functional (our unpublished results), and neither cold sensitive (15°C) nor temperature sensitive (36°C) (unpublished result).

Having met these criteria, we were able to utilize the export assay to compare the nuclear export of mutant and wild-type
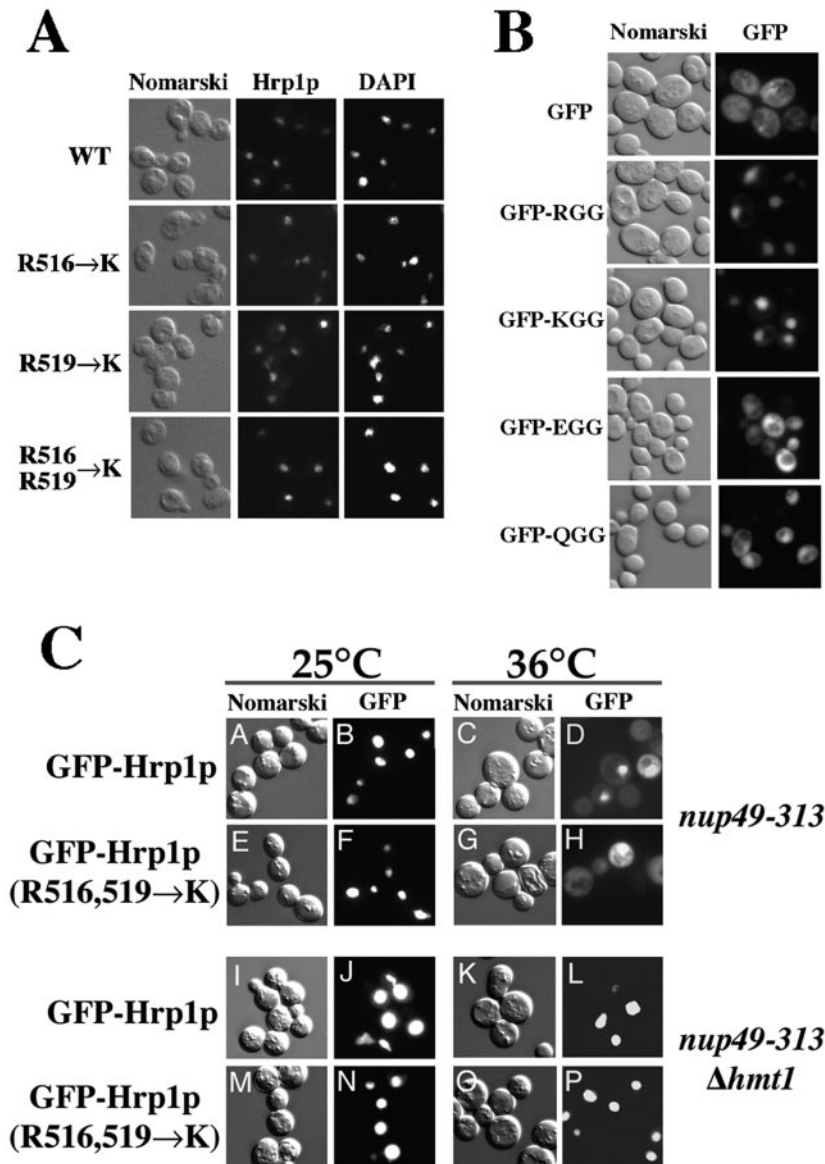
FIG. 3. Hrp1p R→K mutants properly localize to the nucleus and require cellular *HMT1* expression for export. (A) The nuclear localization of Hrp1 RGG→KGG mutant proteins is indistinguishable from that of wild-type Hrp1p. Cells expressing either wild-type (MHY952) or mutant (MHY953, MHY954, or MHY955) Hrp1p were subjected to immunofluorescence microscopy with anti-Hrp1p antibody (middle panels). DNA was visualized with DAPI (right panels), and intact cells were photographed by use of Nomarski optics (left panels). (B) KGG domains serve as functional NLSs. A region of Hrp1p (residues 492 to 534) either carrying a wild-type RGG tripeptide set (HRP1 [492–534]-p12-GFP2) (second row) or harboring KGG (pMHY351) (third row), EGG (pMHY352) (fourth row), or QGG (pMHY353) (fifth row) substitutions was cloned upstream of two plasmid-borne GFP tags. GFP (first row) and GFP chimeras (rows 2 to 5) were visualized in wild-type cells (W303**a**) grown at 30°C. Cells were observed using Nomarski optics (left panels), and GFP was detected by fluorescent microscopy (right panels). (C) Hrp1p (R516,519→K) nuclear export requires *HMT1* expression. Ts⁻ *nup49-313* (panels A to H) and *nup49-313 Δhmt1* (panels I to P) mutant cells expressing either GFP-Hrp1p (panels A to D and I to L) or GFP-Hrp1 (R516/519→K) (panels E to H and M to P) were subjected to the export assay. Cells were incubated at 25°C (left panels) or 36°C (right panels). Living cells were photographed by Nomarski optics or the GFP signal. Strains MHY426, MHY427, MHY428, and MHY429 were examined.

Npl3p in the presence or absence of cellular arginine methylation. GFP-Npl3p accumulated in the cytoplasm of *nup49-313* cells following a shift to 36°C but failed to leave the nucleus in a *nup49-313 Δhmt1* strain, consistent with our previous report that Npl3p nuclear export requires cellular methylation (Fig. 4B, panels D and L) (38). However, the GFP-Npl3 (KGG) fusion protein accumulated in the cytoplasm of both *nup49-313*

cells and *nup49-313 Δhmt1* cells following a shift to 36°C (Fig. 4B, panels H and P). These results demonstrate that Npl3p itself must be arginine methylated to efficiently exit the nucleus, and this requirement for methylation can be bypassed if the Npl3p RGG tripeptides are converted to KGG.

We have previously reported that *Δhmt1* and *npl3-1* alleles are synthetically lethal (15). Given that Npl3 (KGG) nuclear
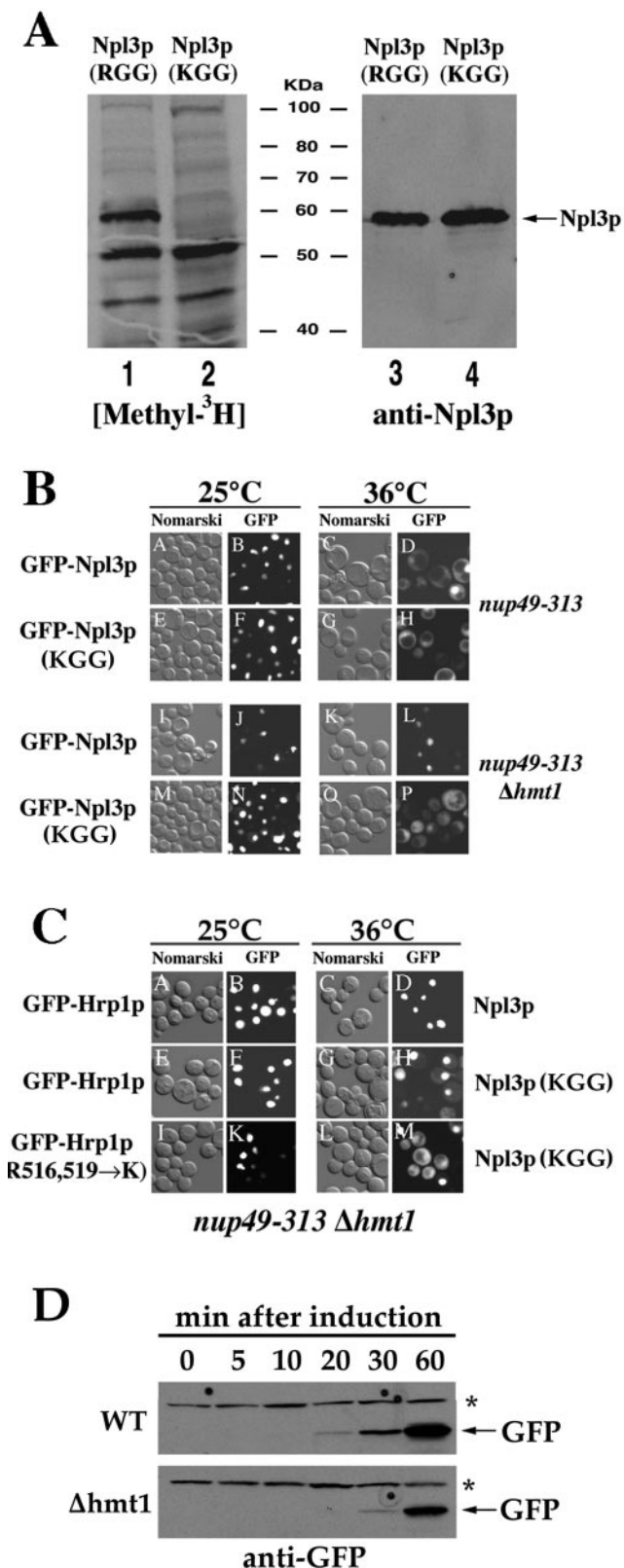
FIG. 4. The export of both Hrp1p and Npl3p is dependent on the methylation state of Npl3p. (A) Npl3p (KGG) is not a substrate for arginine methylation in vivo. Cells expressing either Npl3p (MHY1017, lanes 1 and 3) or Npl3p (KGG) (MHY1120, lanes 2 and

export is methylation independent, we predicted that *npl3* (KGG) expression would rescue the Δ*hmt1 npl3-1* lethal phenotype. To test this hypothesis, a *LEU2* plasmid carrying *npl3* (KGG) was transformed into a *npl3-1* Δ*hmt1* strain covered by a *URA3 HMT1* plasmid. This strain remained viable following loss of the *URA3 HMT1* plasmid by FOA counterselection, indicating rescue of the lethal phenotype (our unpublished results). As controls, a strain carrying the *LEU2* parent vector was found to be nonviable, whereas a *LEU2 NPL3* plasmid rescued the *npl3-1* Δ*hmt1* lethality (our unpublished results).

We postulated that the Hrp1p export block observed in Δ*hmt1* cells may be due not to an absence of Hrp1p methylation but rather to a loss of Npl3p methylation. If true, this interpretation predicts that Npl3 (KGG) expression would relieve the GFP-Hrp1p export block in Δ*hmt1* cells. To test this hypothesis, we compared the nuclear export of GFP-Hrp1 in *nup49-313* Δ*hmt1* cells with that in those expressing Npl3 (KGG). GFP-Hrp1p remained nuclear in cells expressing Npl3p (Fig. 4C, panel D) but accumulated in the cytoplasm of *nup49-313* Δ*hmt1* cells expressing Npl3p (KGG) (Fig. 4C, panel H) after a shift to 36°C. This observation suggests that Npl3p (KGG) permits Hrp1p export in the absence of cellular arginine methylation. Interestingly, the rescue of export is significantly more robust in cells expressing both GFP-HRP1 (R516/519→K) and Npl3 (KGG) (Fig. 4C, panel M), suggesting that Hrp1 methylation may also impact efficient export, but to a lesser extent.

If the methylation of RNPs containing Npl3p is important for its efficient export, the delayed arrival of a nonmethylated RNP might be reflected by delayed mRNA translation. Consistent with this prediction, Western blot analysis detected GFP reporter expression in wild-type cells 20 min after induction, whereas 30 min was required to reach the same level in Δ*hmt1* cells (Fig. 4D). Both strains exhibit equivalent growth

4) were labeled with [*methyl*-³H]SAM as described in Material and Methods. Soluble proteins were resolved by SDS-PAGE and methylation detected by fluorography. (B) Npl3 (KGG) nuclear export is independent of *HMT1* expression. Ts⁻ *nup49-313* (panels A to H) and *nup49-313* Δ*hmt1* (panels I to P) mutant cells expressing either GFP-Npl3p (panels A to D and I to L) or GFP-Npl3p (KGG) (panels E to H and M to P) were subjected to the export assay. Cells were incubated at 25°C (left panels) or 36°C (right panels). Living cells were photographed by Nomarski optics or the GFP signal. Strains MHY418, MHY419, MHY1112, and MHY1113 were used. (C) Npl3p (KGG) expression permits Hrp1p export in the absence of cellular arginine methylation. Ts⁻ *nup49-313* Δ*hmt1* (panels A to H) double-mutant cells harboring plasmids expressing GFP-Hrp1p alone (panels A to D) or transformed with a second plasmid expressing Npl3p (KGG) (panels E to H) were subjected to the export assay. In parallel, the same cells harboring plasmids expressing both GFP-Hrp1 (R516/519→K) and Npl3p (KGG) (panels I to M) were assayed. Cells were incubated at 25°C (left panels) or 36°C (right panels). Living cells were photographed by Nomarski optics or the GFP signal. Strains MHY975, MHY1141, and MHY1142 were assayed. (D) Translation of a GFP reporter is delayed in Δ*hmt1* cells. Wild-type (MHY337; upper panel) and Δ*hmt1* (MHY285; lower panel) shuttling cells expressing *GAL1*-inducible GFP (pCGF-1A) grown at 25°C in raffinose were induced with galactose for the indicated times. Whole lysates were prepared from equal cell numbers, and GFP was detected by immunoblot analysis using anti-GFP antibody. The GFP protein is denoted with an arrow. An asterisk marks a yeast protein that cross-reacts with the anti-GFP antibody.
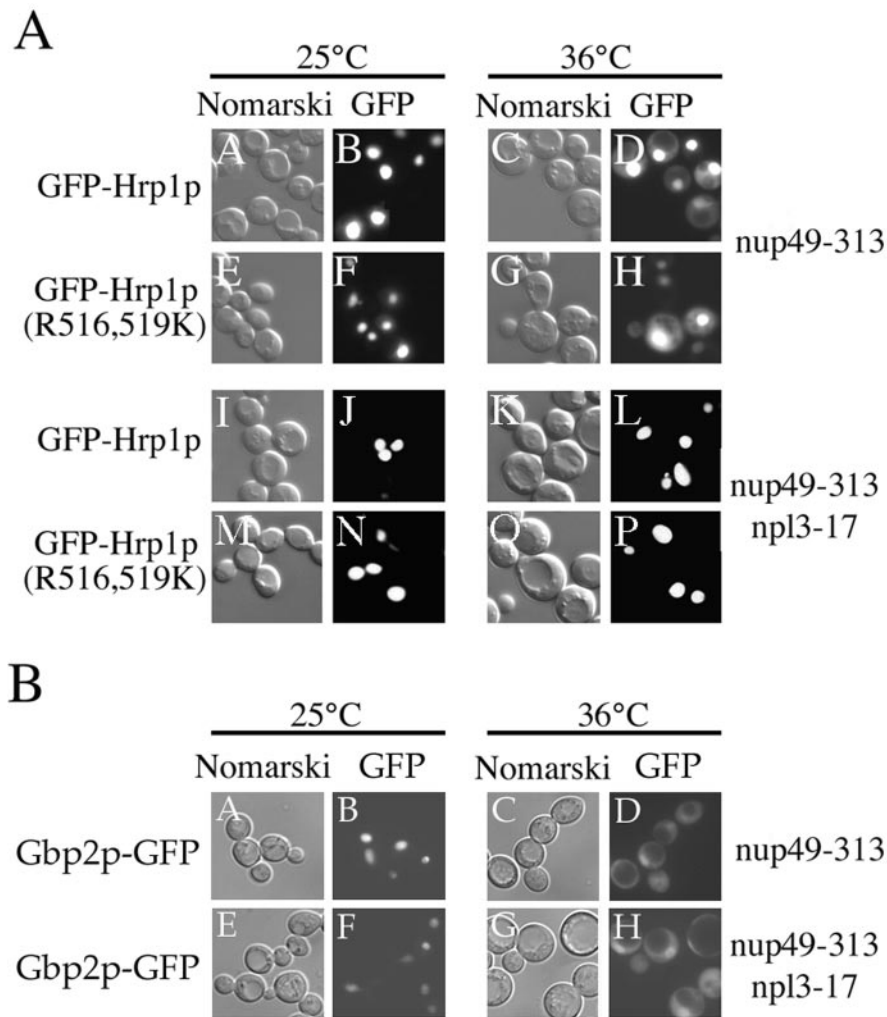
FIG. 5. Hrp1p export is Npl3p dependent. (A) Hrp1-GFP export is blocked in *npl3-17* mutant cells. Ts⁻ *nup49-313* (panels A to H) and *nup49-313 npl3-17* (panels I to P) mutant cells expressing either GFP-Hrp1p (panels A to D and I to L) or GFP-Hrp1 (R516/519→K) (panels E to H and M to P) from a plasmid were subjected to the export assay. Cells were incubated at 25°C (left panels) or 36°C (right panels). Living cells were photographed by Nomarski optics or the GFP signal. Strains MHY426, MHY427, MHY1263, and MHY1265 were used. (B) The Mex67p nuclear export pathway is functional in *npl3-17* cells. *nup49-313* (panels A to D) and *nup49-313 npl3-17* (panels E to H) mutant cells expressing Gbp2p-GFP from a plasmid were subjected to the export assay. Cells were incubated at 25°C (left panels) or 36°C (right panels). Living cells were photographed by Nomarski optics or the GFP signal.

rates in the experimental conditions tested (our unpublished data).

Hrp1p export is Npl3p dependent. Analysis of the Npl3p and Hrp1p (RGG→KGG) mutants supports a model where the export of Hrp1p and that of Npl3p are linked and are dependent upon the methylation state of Npl3p. This model predicts that a specific block in Npl3p export would also inhibit Hrp1p export. To test this hypothesis, we measured the nuclear export of GFP-Hrp1 and that of GFP-Hrp1 (R516/519→K) in *npl3-17* temperature-sensitive cells. Npl3-17 contains two point mutations (F160L and I268T), which, at the restrictive temperature, results in a protein defective in export from the nucleus (25). Both GFP-Hrp1 and GFP-Hrp1 (R516/519→K) accumulated in the cytoplasm of *nup49-313* cells following a shift to 36°C (Fig. 5A, panels D and H) but failed to leave the nucleus in *nup49-313 npl3-17* double-mutant cells (Fig. 5A, panels L and

P), indicating that nuclear export of both wild-type Hrp1p and mutant Hrp1p (R516/519→K) requires Npl3p export.

Because both Hrp1p and Npl3p require the Mex67p mRNA export receptor to leave the nucleus (12), any *NPL3* mutant alleles that inhibited function of this receptor would also result in Hrp1p export defects. To test the fidelity of this pathway in *npl3-17* cells, we monitored the export of another Mex67-dependent protein highly homologous to Npl3p, Gbp2p (42). Analogous to the Hrp1 and Npl3 shuttling proteins, Gbp2 is nuclear at steady-state conditions and nuclear export defects are recognized by the cytoplasmic accumulation of Gbp2 following a block in nuclear import (12). The intracellular localization of a Gbp2-GFP fusion protein was determined by direct immunofluorescence. Consistent with previous reports, Gbp2-GFP accumulates in the cytoplasm of *nup49-313* cells following a shift to 36°C (Fig. 5B, compare panels B and D) (35). Like-

wise, Gbp2-GFP accumulates in the cytoplasm of *nup49-313 npl3-17* double mutants (Fig. 5B, compare panels F and H). In sum, these results suggest that there is not a general export block and, more specifically, that the Mex67 nuclear export pathway utilized by Hrp1p is functional in *npl3-17* cells.

Hrp1p and Npl3p exist in a complex. Because Hrp1p export is Npl3p dependent, we postulated that these two proteins might interact physically. Therefore, we performed Hrp1p immunoprecipitation experiments to isolate endogenous Hrp1p and bound proteins from yeast extracts. We found that a significant amount of Npl3p coimmunoprecipitates with Hrp1 antibodies (Fig. 6A, lane 3). Based upon comparisons to known amounts of recombinant Npl3p (38) and Myc-His$_6$-Hrp1p (14) immunoblotted in parallel (unpublished data), we estimated an Hrp1p/Npl3p molar ratio of 1:1. Interestingly, the amount and ratio of Npl3p precipitated was unaffected in cells either lacking arginine methylation (Fig. 6A, lane 5) or expressing the Hrp1 (R516/519→K) or Npl3p (KGG) mutant proteins (unpublished data). Additionally, we found that this complex formation is not RNA dependent, since Npl3p is still found associated with Hrp1p after incubation with RNase A (Fig. 6A; lanes 4 and 6). These results indicate that Hrp1p and Npl3p are components of the same complex. Significantly, this relationship is independent of RNA and arginine methylation.

RNA binding of Hrp1p and that of Npl3p in vivo are unaffected by cellular arginine methylation. Both Npl3p and Hrp1p bind poly(A)$^+$ RNA in wild-type cells (20, 23, 41, 42). To determine whether the methylation state of these proteins affects this binding, we performed in vivo RNA-protein cross-linking experiments. Wild-type and Δ*hmt1* cells were UV cross-linked, and poly(A)$^+$ complexes were isolated. For each experiment an equal amount of cross-linked RNA was analyzed. Hrp1p and Npl3p present in the original lysate (Fig. 6B, lanes 1, 3, 5, and 7) and eluted from the oligo(dT) column (Fig. 6B, lanes 2, 4, 6, and 8) were detected by immunoblot analysis. In both wild-type and Δ*hmt1* cells, Hrp1p and Npl3p were
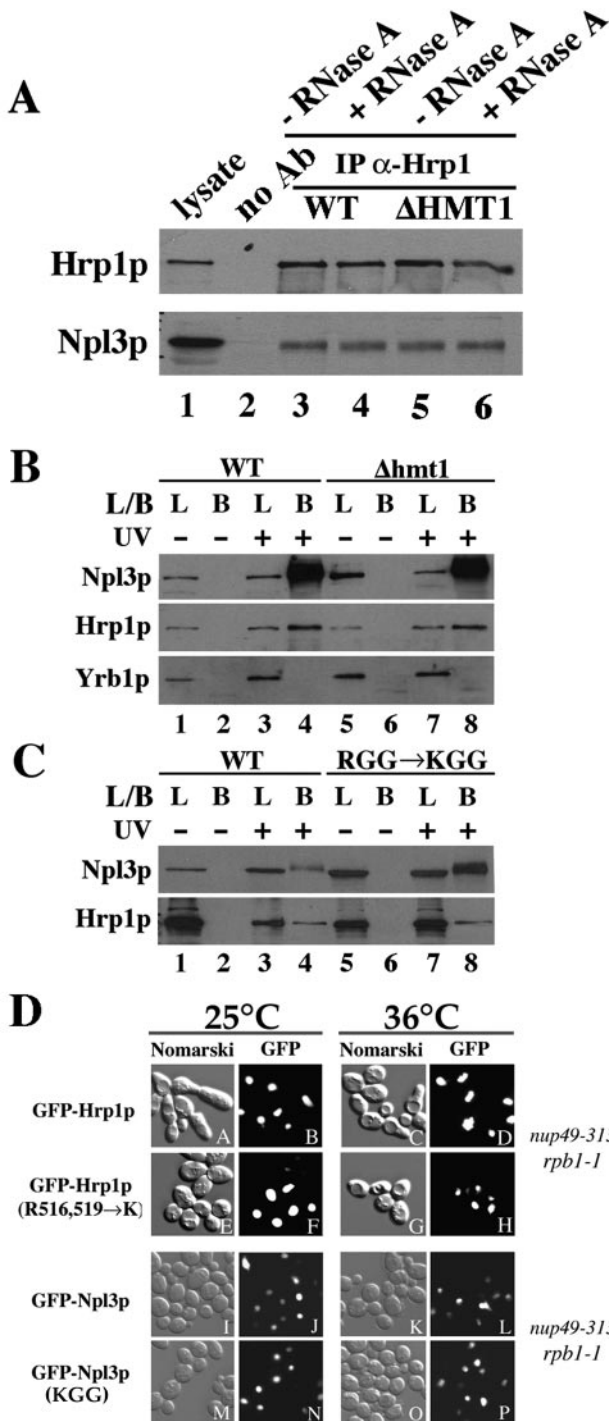
FIG. 6. The methylation state of Npl3p and Hrp1p does not affect mRNA binding or the export requirement for active Pol II transcription. (A) Hrp1p and Npl3p exist in a complex. Hrp1p is immunoprecipitated from cell lysates with Hrp1p antibodies (top). Npl3p coimmunoprecipitates with Hrp1p (bottom). Total lysate is loaded (lane 1). After binding and washing, wild-type (lanes 3 and 4) and Δ*hmt1* (lanes 5 and 6) samples were treated with 50 μg of RNase A/ml in wash buffer (lanes 4 and 6) or wash buffer alone (lanes 3 and 5) and incubated at 30°C for 30 min. Samples were washed once and raised in sample loading buffer, run on an SDS-PAGE gel, and subjected to Western blotting with Hrp1p or Npl3p antibodies. Beads-alone samples were mock immunoprecipitations with protein A-Sepharose (lane 2).

(B) UV cross-linking of Hrp1p and Npl3p to poly(A)$^+$ RNA. Wild-type (WT) and Δ*hmt1* cells expressing either wild-type or (RGG→KGG) variants of Npl3p and Hrp1p were exposed to UV light for cross-linking (+ or − UV irradiation). The lysates were taken before the material was applied to an oligo(dT)-cellulose column. The eluates containing the cross-linked poly(A)$^+$ RNA and bound proteins were treated with RNases. Proteins were analyzed by SDS-PAGE, followed by Western blotting. As a control for nonspecific binding, anti-Yrb1 antibodies were used in a similar experiment. Lanes containing lysates and bound proteins are designated L and B, respectively. (C) UV cross-linking of Hrp1p (R516/519→K) and Npl3p (KGG) mutants to poly(A)$^+$ RNA. Wild-type (lanes 1 to 4, upper and lower panels), Hrp1p (R516/519→K) (lanes 5 to 8, lower panel) and Npl3p (RGG→KGG) (lanes 5 to 8, upper panel) mutants were exposed to UV light for cross-linking (+ or − UV irradiation). Proteins cross-linked to poly(A)$^+$ RNA were monitored as described above. Lanes containing lysates and bound proteins are designated L and B, respectively. (D) Export of Hrp1p and Npl3p (RGG→KGG) mutants is blocked in the absence of RNA Pol II transcription. Double-mutant *nup49-313 rpb1-1* cells (MHY424) expressing GFP-Hrp1p (A to D), GFP-Hrp1p (R516/519→K) (E to H), GFP-Npl3p (I to L), or GFP-Npl3 (KGG) (M to P) were subjected to the export assay. Cells were incubated at 25°C (left panels) or 36°C (right panels). Living cells were photographed by Nomarski optics or for the GFP signal. IP, immunoprecipitation.

detected at equal levels in complex with poly(A)$^+$ RNA (Fig. 6B, lanes 4 and 8). The strong binding of both proteins to mRNA is specific, since binding of a cytoplasmic non-RNA-binding protein, Yrb1, to poly(A)$^+$ RNA could not be detected (Fig. 6B, lanes 4 and 8). We did not observe nonspecific protein binding to the oligo(dT) column when UV cross-linking was not performed prior to the isolation of poly(A)$^+$ RNA (Fig. 6B, lanes 2 and 6). Together the data indicate RNA binding of Hrp1p and that of Npl3p are unaffected by cellular arginine methylation.

We also examined the impact of RGG→KGG substitutions on Hrp1p and Npl3p RNA binding in vivo (Fig. 6C). Although these amino acid substitutions did not impact the level of cross-linked Hrp1p (Fig. 6C, lanes 4 and 8), more Npl3p (KGG) was detected in complex with poly(A)$^+$ RNA than wild-type Npl3p (Fig. 6C, compare lanes 4 and 8). In contrast, the levels of cross-linked Hrp1p and Npl3p were unaffected in cells expressing Npl3p (KGG) or Hrp1p (R516,519K), respectively (our unpublished results). In sum, these results suggest that the Npl3p (KGG) mutant exhibits increased RNA binding in vivo independently of the methylation state of Hrp1p. However, it should be noted that these assays do not distinguish between direct and indirect RNA binding effects.

The nuclear export of the Hrp1 and Npl3 (RGG→KGG) mutants requires ongoing RNA synthesis. Because the nuclear export of wild-type Hrp1p and that of wild-type Npl3p are intimately tied to ongoing RNA synthesis (25, 38), we tested whether the same is true for the Hrp1 and Npl3 (RGG→KGG) mutants. To accomplish this, we employed a temperature-sensitive allele of RNA polymerase II (Pol II), termed *rpb1-1* (30). In the *rpb1-1* strains, RNA Pol II transcription is inhibited at the nonpermissive temperature. The nuclear export assay was performed with a strain containing both the *nup49-313* and *rpb1-1* mutant alleles (25). As expected, Hrp1p and Npl3p GFP fusions failed to exit the nucleus in this strain at the nonpermissive temperature (Fig. 6D, panels D and L) (25). Significantly, the Hrp1p and Npl3p (RGG→KGG) GFP fusions also failed to accumulate in the cytoplasm (Fig. 6D, panels H and P) at the nonpermissive temperature. This result is not attributable to a lack of protein synthesis, because when the assay was performed in the presence or absence of the protein synthesis inhibitor cycloheximide, GFP-Hrp1p and GFP-Hrp1p (R516/519→K) accumulated in the cytoplasm at equal levels (our unpublished results). These results indicate that RNA Pol II transcription, but not new protein synthesis, is required for export of Hrp1p and Npl3p (RGG→KGG) GFP fusions. In addition, these results suggest that the mutant proteins are exiting the nucleus associated with mRNA.

DISCUSSION

In this report we have investigated the effect of arginine methylation on the nuclear export of two hnRNPs, Hrp1p and Npl3p. Although previous studies have shown that this modification is critical for the efficient export of these hnRNPs, it has remained uncertain whether this modification affects each substrate directly or through its effects on other proteins. To test whether arginine methylation directly impacts Hrp1p export, we mapped the modified residues to R516 and R519

within the RGG domain and examined the functional consequences of substituting lysines at these positions. By use of a nuclear export assay, the ability of Hrp1p to efficiently exit the nucleus was shown to require cellular methyltransferase activity, but the modification of Hrp1p itself was dispensable. We further demonstrate that Npl3 arginine methylation not only facilitates its own export but also is required for Hrp1p to efficiently exit the nucleus. Hrp1p and Npl3p exist in an RNP complex whose export is dependent on the presence of methylated Npl3p.

We propose a working model in which Hrp1p and Npl3 exit the nucleus as components of the same RNP complex. Efficient export of this complex requires masking RGG tripeptides contained within Npl3p, either by arginine methylation or by amino acid substitution. In both scenarios, Hrp1p and Npl3p retain the ability to bind mRNA and require ongoing transcription for nuclear export. However, if the RGG tripeptides within Npl3p are unmodified, both Hrp1 and Npl3p export the nucleus less efficiently. The mechanism of this retention is unclear but does not appear to result from a decreased mRNA affinity of these proteins. Conditions that could hinder export include the inability to generate an export-competent RNP or decreased interaction with the export machinery. This preliminary model is easily testable and should serve to guide future experiments.

Surprisingly, the methylation state of Hrp1p appears to have no discernible effect on the export of its RNP complex in our assays. However, this result is open to interpretation, since the methylation level of the RNP complex as a whole, rather than the methylation of individual proteins, may dictate efficient export. If this is the case, Npl3 would be expected to have a stronger influence, since it contains 15 RGG tripeptides compared to only two found within Hrp1p. In such a scenario, a partial RNP complex retention due to unmodified RGG tripeptides within Hrp1p might not be detected in our export assay. This idea is consistent with the observation that non-methylated Hrp1p (R516/519→K) is exported more efficiently in Δ*hmt1* cells expressing nonmethylated Npl3p (KGG). Alternatively, arginine-methylated proteins may share an underlying biochemical function (i.e., protein binding) that differentially impacts the cellular roles of these enzymes (i.e., 3′-end maturation, nuclear export, nonsense-mediated decay). If true, the loss of Hrp1p methylation may impact another aspect of RNA maturation.

Given that Hrp1p and Npl3p are components of an RNP whose export is dependent on the methylation state of Npl3p, the cytoplasmic accumulation of Hrp1p in Δ*hmt1* cells expressing Npl3 (KGG) might be expected to be similar to that of Npl3 (KGG). However, the extent of GFP-Hrp1p export (Fig. 4C, panel H) was less than that observed for GFP-Npl3 (KGG) (Fig. 4B, panel P). One interpretation of this result is that Hrp1p is also a component of other RNPs, not associated with Npl3p. Alternatively, export efficiency could be influenced by the endogenous expression of wild-type unmethylated Npl3p in theses cells, which could compete for RNP complex formation with epitope-expressed Npl3 (KGG).

Previous studies have found that RGG domains located within Hrp1p and Npl3p serve as functional nuclear localization signals by interacting with the Kap104 and Mtr10 nuclear import receptors, respectively (24, 37). Because the nuclear

export assay relies on monitoring the appearance of a target protein in the cytoplasm, a prerequisite for our use of the assay was that conserved R-to-K substitutions within the RGG domains of Npl3p and Hrp1p would not alter steady-state nuclear localization. Interestingly, we found the nuclear localization of both proteins to be unaffected by these substitutions. Additional experiments utilizing glutamine and glutamate substitutions within Hrp1 were found to disrupt the nuclear import. In sum, these experiments argue that a basic charge is important at this position of the signal but the arginine residue itself is not required.

Given that lysines and arginines are both positively charged residues and structurally similar, it has been an open question whether the Hmt1 enzyme could modify a lysine residue if placed in the proper context. Although we and others have shown that synthetic peptides containing KGG repeats are not modified in vitro by arginine methylation reactions (22), in the case of Hrp1, the placement of lysine residues within the context of a consensus sequence resulted in a protein which was functional but could no longer be methylated. Due to the lack of sensitivity of our in vivo assay, we cannot rule out the possibility of methylation below our level of detection.

It has been proposed that Nab2p interacts with an unknown nuclear protein that retains unmethylated Nab2p in the nucleus (27). However, this model was based on a mutant with a deletion of the entire RGG domain, and it was not determined whether this mutant is also dependent on cellular arginine methylation for export. Therefore, it is not known whether methylation of Nab2p itself is necessary for its export or, like Hrp1p, its export is dependent on the methylation state of Npl3p. We have shown that an Npl3 mutant can efficiently export in the absence of all other arginine methylation and carry an Hrp1p-containing RNP to the cytoplasm. Nab2p also complexes with Npl3p (our unpublished data). Therefore, Nab2p may also be dependent on Npl3p for efficient export, and retention of Nab2p in the absence of cellular methylation may be an indirect effect.

Nevertheless, we believe it is possible that a nuclear factor that interacts with unmethylated RGG motifs could specifically retain RNPs containing these proteins in the nucleus. We prefer a hypothesis in which RNPs containing unmethylated Npl3p fail to acquire the appropriate complement of proteins necessary for efficient export. This would suggest a common biochemical property of RGG proteins: that methylated RGGs allow remodeling of RNPs as they transit through RNA processing and export. Defects due to a lack of RGG methylation would be manifested differently depending on each protein's role in RNA maturation.

Does cellular arginine methylation facilitate the nuclear export of all hnRNPs receiving this modification? We know that the Hrp1, Nab2, and Npl3 shuttling proteins, either directly or indirectly, require arginine methylation for export (11, 38). However, two additional shuttling hnRNP proteins of yeast containing RGG tripeptides have been reported, Hrb1 and Gbp2, whose export is unaffected by loss of the arginine methyltransferase (38, 42). At present, this question remains unresolved. One possibility is that these proteins exit the nucleus independently of Npl3p. Alternatively, Hrb1p and Gbp2p may not be arginine methylated in the cell. Although both proteins

contain minimal RGG motifs, neither has been shown to be a substrate for arginine methylation in vivo.

REFERENCES

1. **Beyer, A. L., M. E. Christensen, B. W. Walker, and W. M. LeStourgeon.** 1977. Identification and characterization of the packaging proteins of core 40S hnRNP particles. Cell **11:**127–138.
2. **Boeke, J. D., F. LaCroute, and G. R. Fink.** 1984. A positive selection for mutants lacking orotidine-5′-phosphate decarboxylase activity in yeast: 5-fluoro-orotic acid resistance. Mol. Gen. Genet. **197:**345–346.
3. **Bossie, M. A., C. DeHoratius, G. Barcelo, and P. Silver.** 1992. A mutant nuclear protein with similarity to RNA binding proteins interferes with nuclear import in yeast. Mol. Biol. Cell **3:**875–893.
4. **Doye, V., R. Wepf, and E. C. Hurt.** 1994. A novel nuclear pore protein Nup133p with distinct roles in poly(A)+ RNA transport and nuclear pore distribution. EMBO J. **13:**6062–6075.
5. **Dreyfuss, G., V. N. Kim, and N. Kataoka.** 2002. Messenger-RNA-binding proteins and the messages they carry. Nat. Rev. Mol. Cell Biol. **3:**195–205.
6. **Gary, J. D., W. J. Lin, M. C. Yang, H. R. Herschman, and S. Clarke.** 1996. The predominant protein-arginine methyltransferase from Saccharomyces cerevisiae. J. Biol. Chem. **271:**12585–12594.
7. **Gietz, D., A. St Jean, R. A. Woods, and R. H. Schiestl.** 1992. Improved method for high efficiency transformation of intact yeast cells. Nucleic Acids Res. **20:**1425.
8. **Gilbert, W., and C. Guthrie.** 2004. The Glc7p nuclear phosphatase promotes mRNA export by facilitating association of Mex67p with mRNA. Mol. Cell **13:**201–212.
9. **Gonzalez, C. I., M. J. Ruiz-Echevarria, S. Vasudevan, M. F. Henry, and S. W. Peltz.** 2000. The yeast hnRNP-like protein Hrp1/Nab4 marks a transcript for nonsense-mediated mRNA decay. Mol. Cell **5:**489–499.
10. **Gratzer, S., T. Beilharz, T. Beddoe, M. F. Henry, and T. Lithgow.** 2000. The mitochondrial protein targeting suppressor (mts1) mutation maps to the mRNA-binding domain of Npl3p and affects translation on cytoplasmic polysomes. Mol. Microbiol. **35:**1277–1285.
11. **Green, D. M., K. A. Marfatia, E. B. Crafton, X. Zhang, X. Cheng, and A. H. Corbett.** 2002. Nab2p is required for poly(A) RNA export in Saccharomyces cerevisiae and is regulated by arginine methylation via Hmt1p. J. Biol. Chem. **277:**7752–7760.
12. **Hacker, S., and H. Krebber.** 2004. Differential export requirements for shuttling serine/arginine-type mRNA-binding proteins. J. Biol. Chem. **279:** 5049–5052.
13. **Henry, M., C. Z. Borland, M. Bossie, and P. A. Silver.** 1996. Potential RNA binding proteins in Saccharomyces cerevisiae identified as suppressors of temperature-sensitive mutations in NPL3. Genetics **142:**103–115.
14. **Henry, M. F., D. Mandel, V. Routson, and P. A. Henry.** 2003. The yeast hnRNP-like protein Hrp1/Nab4 accumulates in the cytoplasm after hyperosmotic stress: a novel Fps1-dependent response. Mol. Biol. Cell **14:**3929–3941.
15. **Henry, M. F., and P. A. Silver.** 1996. A novel methyltransferase (Hmt1p) modifies poly(A)+-RNA-binding proteins. Mol. Cell. Biol. **16:**3668–3678.
16. **Hill, J. E., A. M. Myers, T. J. Koerner, and A. Tzagoloff.** 1986. Yeast/E. coli shuttle vectors with multiple unique restriction sites. Yeast **2:**163–167.
17. **Ito, H., Y. Fukuda, K. Murata, and A. Kimura.** 1983. Transformation of intact yeast cells treated with alkali cations. J. Bacteriol. **153:**163–168.
18. **Kahana, J. A., and P. A. Silver.** 1996. Use of the A. victoria green fluorescent protein to study protein dynamics in vivo, p. 9.6.13–9.6.19. In F. M. Ausubel, R. Brent, R. E. Kingston, D. E. Moore, J. G. Seidman, J. A. Smith, and K. Struhl (ed.), Current protocols in molecular biology, vol. 1. John Wiley & Sons, New York, N.Y.
19. **Kassir, Y., and G. Simchen.** 1991. Monitoring meiosis and sporulation in Saccharomyces cerevisiae. Methods Enzymol. **194:**94–110.
20. **Kessler, M. M., M. F. Henry, E. Shen, J. Zhao, S. Gross, P. A. Silver, and C. L. Moore.** 1997. Hrp1, a sequence-specific RNA-binding protein that shuttles between the nucleus and the cytoplasm, is required for mRNA 3′-end formation in yeast. Genes Dev. **11:**2545–2556.
21. **Kim, S., B. M. Merrill, R. Rajpurohit, A. Kumar, K. L. Stone, V. V. Papov, J. M. Schneiders, W. Szer, S. H. Wilson, W. K. Paik, and K. R. Williams.** 1997. Identification of N(G)-methylarginine residues in human heterogeneous RNP protein A1: Phe/Gly-Gly-Gly-Arg-Gly-Gly-Gly/Phe is a preferred recognition motif. Biochemistry **36:**5185–5192.
22. **Klein, S., J. A. Carroll, Y. Chen, M. F. Henry, P. A. Henry, I. E. Ortonowski,**

G. Pintucci, R. C. Beavis, W. H. Burgess, and D. B. Rifkin. 2000. Biochemical analysis of the arginine methylation of high molecular weight fibroblast growth factor-2. J. Biol. Chem. 275:3150–3157.

23. Krebber, H., T. Taura, M. S. Lee, and P. A. Silver. 1999. Uncoupling of the hnRNP Npl3p from mRNAs during the stress-induced block in mRNA export. Genes Dev. 13:1994–2004.

24. Lee, D. C., and J. D. Aitchison. 1999. Kap104p-mediated nuclear import. Nuclear localization signals in mRNA-binding proteins and the role of Ran and Rna. J. Biol. Chem. 274:29031–29037.

25. Lee, M. S., M. Henry, and P. A. Silver. 1996. A protein that shuttles between the nucleus and the cytoplasm is an important mediator of RNA export. Genes Dev. 10:1233–1246.

26. Liu, Q., and G. Dreyfuss. 1995. In vivo and in vitro arginine methylation of RNA-binding proteins. Mol. Cell. Biol. 15:2800–2808.

27. Marfatia, K. A., E. B. Crafton, D. M. Green, and A. H. Corbett. 2003. Domain analysis of the Saccharomyces cerevisiae heterogeneous nuclear ribonucleoprotein, Nab2p. Dissecting the requirements for Nab2p-facilitated poly(A) RNA export. J. Biol. Chem. 278:6731–6740.

28. Minvielle-Sebastia, L., K. Beyer, A. M. Krecic, R. E. Hector, M. S. Swanson, and W. Keller. 1998. Control of cleavage site selection during mRNA 3′ end formation by a yeast hnRNP. EMBO J. 17:7454–7468.

29. Najbauer, J., B. A. Johnson, A. L. Young, and D. W. Aswad. 1993. Peptides with sequences similar to glycine, arginine-rich motifs in proteins interacting with RNA are efficiently recognized by methyltransferase(s) modifying arginine in numerous proteins. J. Biol. Chem. 268:10501–10509.

30. Nonet, M., C. Scafe, J. Sexton, and R. Young. 1987. Eucaryotic RNA polymerase conditional mutant that rapidly ceases mRNA synthesis. Mol. Cell. Biol. 7:1602–1611.

31. Rawal, N., R. Rajpurohit, M. A. Lischwe, K. R. Williams, W. K. Paik, and S. Kim. 1995. Structural specificity of substrate for S-adenosylmethionine:protein arginine N-methyltransferases. Biochim. Biophys. Acta 1248:11–18.

32. Rose, M. D., F. Winston, and P. Hieter (ed.). 1990. Methods in yeast genetics: a laboratory course manual. Cold Spring Harbor Laboratory, Cold Spring Harbor, N.Y.

33. Sadler, I., A. Chiang, T. Kurihara, J. Rothblatt, J. Way, and P. Silver. 1989. A yeast gene important for protein assembly into the endoplasmic reticulum and the nucleus has homology to DnaJ, an Escherichia coli heat shock protein. J. Cell Biol. 109:2665–2675.

34. Scherer, S., and R. W. Davis. 1979. Replacement of chromosome segments with altered DNA sequences constructed in vitro. Proc. Natl. Acad. Sci. USA 76:4951–4955.

35. Schlenstedt, G., C. Saavedra, J. D. Loeb, C. N. Cole, and P. A. Silver. 1995. The GTP-bound form of the yeast Ran/TC4 homologue blocks nuclear protein import and appearance of poly(A)+ RNA in the cytoplasm. Proc. Natl. Acad. Sci. USA 92:225–229.

36. Scott, H. S., S. E. Antonarakis, M. D. Lalioti, C. Rossier, P. A. Silver, and M. F. Henry. 1998. Identification and characterization of two putative human arginine methyltransferases (HRMT1L1 and HRMT1L2). Genomics 48: 330–340.

37. Senger, B., G. Simos, F. R. Bischoff, A. Podtelejnikov, M. Mann, and E. Hurt. 1998. Mtr10p functions as a nuclear import receptor for the mRNA-binding protein Npl3p. EMBO J. 17:2196–2207.

38. Shen, E. C., M. F. Henry, V. H. Weiss, S. R. Valentini, P. A. Silver, and M. S. Lee. 1998. Arginine methylation facilitates the nuclear export of hnRNP proteins. Genes Dev. 12:679–691.

39. Shen, E. C., T. Stage-Zimmermann, P. Chui, and P. A. Silver. 2000. The yeast mRNA-binding protein Npl3p interacts with the cap-binding complex. J. Biol. Chem. 275:23718–23724.

40. Sikorski, R. S., and P. Hieter. 1989. A system of shuttle vectors and yeast host strains designed for efficient manipulation of DNA in Saccharomyces cerevisiae. Genetics 122:19–27.

41. Wilson, S. M., K. V. Datar, M. R. Paddy, J. R. Swedlow, and M. S. Swanson. 1994. Characterization of nuclear polyadenylated RNA-binding proteins in Saccharomyces cerevisiae. J. Cell Biol. 127:1173–1184.

42. Windgassen, M., and H. Krebber. 2003. Identification of Gbp2 as a novel poly(A)+ RNA-binding protein involved in the cytoplasmic delivery of messenger RNAs in yeast. EMBO Rep. 4:278–283.

43. Xu, C., P. A. Henry, A. Setya, and M. F. Henry. 2003. In vivo analysis of nucleolar proteins modified by the yeast arginine methyltransferase Hmt1/Rmt1p. RNA 9:746–759.